Battelle

Final Report No. 13-021

Final Report

Predicting Times to Failure for ERW Seam Defects that Grow by Pressure-Cycle-Induced Fatigue

J. F. Kiefner and K. M. Kolovich

January 28, 2013

Kiefner & Associates, Inc.
585 Scherers Court
Worthington, Ohio 43085

(614) 888-8220
www.kiefner.com

0533-1101

Intentionally blank

Final Report No. 13-021

Final Report

on

PREDICTING TIMES TO FAILURE FOR ERW SEAM DEFECTS THAT GROW BY PRESSURE-CYCLE-INDUCED FATIGUE

to

BATTELLE

AS THE DELIVERABLE OF SUBTASK 2.5 ON
U.S. DEPARTMENT OF TRANSPORTATION
OTHER TRANSACTION AGREEMENT NO. DTPH56-11-T-000003

January 28, 2013

by

J. F. Kiefner and K. M. Kolovich

Kiefner and Associates, Inc.
585 Scherers Court
Worthington, Ohio 43085

0533-1101

DISCLAIMER

This document presents findings and/ or recommendations based on engineering services performed by employees of Kiefner and Associates, Inc. The work addressed herein has been performed according to the authors' knowledge, information, and belief in accordance with commonly accepted procedures consistent with applicable standards of practice, and is not a guaranty or warranty, either expressed or implied.

The analysis and conclusions provided in this report are for the sole use and benefit of the Client. No information or representations contained herein are for the use or benefit of any party other than the party contracting with Kiefner. The scope of use of the information presented herein is limited to the facts as presented and examined, as outlined within the body of this document. No additional representations are made as to matters not specifically addressed within this report. Any additional facts or circumstances in existence but not described or considered within this report may change the analysis, outcomes and representations made in this report.

EXECUTIVE SUMMARY

The work described herein is part of a comprehensive study of ERW seam integrity and its impact on pipeline safety. The objective of this part of the work is to identify appropriate means for predicting the remaining lives of defects that remain after a seam integrity assessment and that may become enlarged by pressure-cycle-induced fatigue. Predictions of remaining lives of defects are needed so that re-assessment or remediation can be carried out in a timely manner to prevent such defects from growing large enough to fail in service.

Pressure-cycle-induced fatigue crack growth of ERW seam defects is a recognized threat to the integrity of a hazardous liquid pipeline. Pressure-cycle-induced fatigue failures are not believed to be a near-term threat to natural gas pipelines because of their less-frequent and lower-amplitude pressure cycles. But, whatever the timing, the threat of failure from pressure-cycle-induced fatigue can be addressed by periodic ERW seam-integrity assessment. Seam integrity assessment can be accomplished either by hydrostatic testing or by in-line inspection (ILI) using a suitable crack-detection tool. This document discusses the analytical tools that facilitate predicting the timing of ERW seam-integrity assessments to prevent service failures from defects that might be growing in response to pressure-cycle-induced fatigue.

Scheduling retesting or remediation via fatigue-crack-growth analysis involves establishing the initial sizes of defects, applying representative operational pressure cycles to cause the defects to grow, and determining the number of pressure cycles required to cause the defects to attain (final) sizes that will cause a failure at the maximum operating pressure (MOP) of the pipeline. The number of pressure cycles required to grow the initial defects to failure corresponds to a certain period of time, so the output of the analysis is a time to failure for each defect considered. A factor of safety is then applied to the time to failure so that a response is made well before any growing defect can reach a size that would cause failure at the MOP.

Defects that remain after a hydrostatic test can be no larger than the size that would have caused a hydrostatic test failure, so the maximum test pressure is used to establish the initial sizes of a representative sample of defects with different length-depth combinations that could have barely survived the test. The minimum time to failure for the worst-case defect modified by the factor of safety determines when hydrostatic retesting is needed to assure seam integrity.

In the case of defects identified by ILI, their locations and initial sizes will be known. The time to failure for each defect can be predicted, and a remedial response can be undertaken in a timely manner for each defect based on its predicted time to failure modified by the factor of safety.

This study has shown that times to failure after a hydrostatic test can be calculated via a Paris-law approach, provided that the user is able to supply the relevant data that includes pipe geometry and strength level, the relevant operating pressure-cycle spectrum and test pressure history for the segment being assessed. Other factors that affect the times to failures include material toughness, flow stress, and the crack growth rate constants associated with the Paris-law equation. These latter factors will not be known for each and every piece of pipe in a pipeline. However, the sensitivity analysis shows that the analyst can expect to obtain conservative estimates of times to failure after a hydrostatic test by assuming a toughness level corresponding to a full-size-equivalent Charpy upper-shelf energy level of 200 ft lb and a flow stress equal to the minimum specified ultimate tensile strength of the base metal[1]. Experience shows that the crack growth rate constants found in the API 579 standard for fitness-for-service are acceptable. Lastly, a factor of safety of 2 should be applied to the calculated times to failure to account for uncertainties in the material properties and the calculation process.

In using fatigue analysis to calculate the times to failure after a hydrostatic test, it must be assumed that defects could exist anywhere along the pipeline that are severe enough to have failure pressures no higher than that of the hydrostatic test pressure. This means that the analyst may have to calculate times to failure for multiple points along the pipeline taking account of the test level applied at each location, the wall thickness at each location, the effect of the hydraulic gradient on the pressure cycles at each location, and the effect of elevation on the static head at each location.

The sensitivity study further shows that the calculated times to failure after a hydrostatic test increase exponentially with increasing test-pressure-to-operating-pressure ratio. Therefore, the operator can maximize the length of time between retests by utilizing the highest feasible test pressure that will not cause significant permanent expansion of pipe or an intolerable number of test failures. In absolute terms, the higher the test stress relative to the specified minimum yield strength of the pipe, the smaller the remaining defects will be. Smaller remaining defects mean longer times to failure after the test. For that reason, for a pipeline that is operated at maximum stress levels below 72% of SMYS, the test-pressure-to-operating-pressure ratio must be greater than that applied on a pipeline that operates at 72% of SMYS to achieve the same time to failure as that for the pipeline that operates at 72% of SMYS.

The sensitivity study also addressed the parameters that affect the calculated times to failure after a seam integrity assessment via an ILI crack-detection tool. In a manner similar to that used to

[1] The purpose of using the unusually high level of Charpy energy and a high value of flow stress (equal to the ultimate tensile strength) is to calculate the largest possible defects that could have survived a given level of hydrostatic test. The resulting "maximum-size" defects lead to the shortest predicted times to failure.

calculate times to failure after a hydrostatic test, times to failure after an ILI seam integrity assessment can be estimated using a Paris-law approach. For an analysis following seam assessment by ILI, the analyst must know the pipe geometry and strength level, and the relevant operating pressure-cycle spectrum for the segment being assessed. In the case of assessment by ILI (unlike in the case of a hydrostatic test), it is prudent to assume a low value of toughness because the lower the toughness used in the analysis is, the lower the failure stress of a given defect will be and the shorter will be the predicted times to failure. A toughness level corresponding to a full-size-equivalent Charpy upper shelf energy level of 15 ft lb would seem to be an appropriate value because that is about the minimum value one can expect for the base metal of a line pipe material manufactured prior to 1980.

Also, unlike in the case of a hydrostatic test, it is prudent to assume a low value of flow stress because the lower the flow stress used in the analysis is, the shorter will be the predicted times to failure after the test. An appropriate level of flow stress would be SMYS+10,000 psi.

As in the case involving predicting times to failure after a hydrostatic testing, the crack growth rate constants found in the API 579 standard for fitness-for-service are acceptable for use in calculating times to failure after a seam assessment via ILI.

In using fatigue analysis to calculate the time to failure after a seam integrity assessment via ILI, the pipeline operator will know where defects that could grow by fatigue are located and should also be able to tell within certain bounds, the lengths and depths of the defects. Since the locations of the anomalies are known in the case of assessment by ILI, it is simply a matter of adjusting the pressure-cycle spectrum from the upstream and active downstream stations to account for the distance along the hydraulic gradient. An analysis should be made for all significant anomalies so that the times to failure will be known. The operator will then be able to prioritize the anomalies by their times to failure and respond in a timely manner to remediate them before they grow to a size that would cause an in-service failure.

Assessment of ERW seam integrity using a reliable ILI crack-detection tool should permit longer intervals between re-assessments than is the case with repeated hydrostatic testing because an ILI tool should be able to find much smaller defects than those that can survive a hydrostatic test to the highest feasible test stress levels.

The sensitivity study reveals that errors in tool-called depth and/or in tool-called length can significantly alter the predicted time to failure. In cases where the times to failure were calculated for the tool-called depths and for depths 10% deeper than the tool-called depths, the times to failure were 26% to 42% shorter for the 10%-deeper defects depending on the depth/thickness ratio of the defect. In cases where times to failure were calculated for tool-called

lengths and for lengths 25% longer than the tool-called lengths, the times to failure were 37% to 42% shorter for the 25%-longer defects depending on the length of the defect. Because tool error may cause uncertainty as to the actual length and depth of an anomaly, the pipeline operator should take such uncertainty into account by applying a suitable factor of safety to the calculated times to failure. As will be discussed, applying a factor of safety of 2 with some additional conservatism built in (e.g., assuming the deepest depth in the bracket, adding a specific tool tolerance) would seem to be satisfactory.

TABLE OF CONTENTS

LIST OF FIGURES

LIST OF TABLE

Intentionally blank

Predicting Times to Failure for ERW Seam Defects that Grow by Pressure-Cycle-Induced Fatigue

J. F. Kiefner and K. M. Kolovich

INTRODUCTION

This document presents a description of how one might estimate either the frequency with which ERW seam integrity should be assessed by hydrostatic testing or the time the remediation of defects discovered through in-line inspection must be done in order to prevent in-service failures from defects that may be growing by pressure-cycle-induced fatigue.

BACKGROUND

Experience shows that pipelines have failed in service as the result of pressure-cycle-induced fatigue crack growth initiating at various types of ERW seam defects. Some of these failures were described in another report on this same project[i.] All of the fatigue failures documented in Reference 1 occurred in hazardous liquid pipelines. The absence of evidence of such failures occurring in natural gas pipelines is believed to be the result of the difference in pressure-cycle intensity between the two types of pipelines. It is possible that, eventually, the phenomenon will show up in natural gas pipelines after very long periods of service, but to date there are few, if any, documented cases of failures in gas pipelines from pressure-cycle-induced fatigue.

Because ERW seam defects that are too small to fail in a hydrostatic test or are not remediated after an assessment by ILI crack-detection technology may become enlarged by pressure-cycle-induced fatigue, operators of hazardous liquid pipeline need to periodically re-assess the integrity of their ERW pipelines. A rational basis for scheduling such re-assessments should consist of estimating the time to failure for the worst-case remaining defect and employ a safety factor to schedule the re-assessment or remediation well before that defect has time to grow to failure at the operating pressure.

In the following section of this report, the most commonly-used technology for modeling fatigue crack growth is discussed, the attributes and operational characteristics of pipelines that influence pressure-cycle-induced fatigue are discussed, and a proprietary software model that adapts fatigue-crack-growth technology to pipelines is exercised to show how a pipeline operator could rationally estimate the time to failure for the worst-case surviving defects in a particular pipeline.

PREDICTING FATIGUE CRACK GROWTH

The Technology

A commonly-used basis for fatigue crack growth modeling is the "Paris-law" approach named after its principal developer[ii]. The Paris-law equation is generally written as follows.

$$\frac{da}{dN} = C(\Delta K)^n \qquad \textbf{Equation 1}$$

where:
da/dN is an increment of crack growth, *inch/cycle*
C and *n* are constants for a particular material and environment
ΔK is the change in stress intensity factor at the tip of the fatigue crack during a cycle of changing applied stress, $psi\sqrt{inch}$

ΔK is calculated using the Raju/Newman equation[iii] which has the form:

$$\Delta K = F\Delta\sigma\sqrt{\pi a} \qquad \textbf{Equation 2}$$

where:

F is a constant that depends on the shape of the stressed element, the ratio of defect depth to wall thickness, the ratio of defect depth to defect length, and the position of the tip of the crack
Δσ is the change in stress during a cycle of loading and unloading, psi
a is the depth of a part-through-wall crack, inch

The number of cycles of a given level of stress needed for a crack with an initial depth, a_i to grow to a final depth a_f is calculated by integrating Equation 1. Because of the complexity associated with most practical structures, closed-form integration of Equation 1 is usually not possible, and software designed for the purpose of numerical integration is generally used to perform the integration and calculate cycles to failure. The software models available for calculating cycles to failure also must be able to count cycles with variable stress ranges because most real loading situations involve load applications that vary with time. Various cycle-counting schemes are presented in ASTM 1049-85 (2011)e1, and the one used in the analyses described in this report is called "rainflow" counting.

Application of Fatigue Crack Growth Technology to Pipelines

Overview

When the objective of a fatigue analysis is to estimate the remaining life of defects that could have just barely survived a particular hydrostatic test, one must realize that there is an infinite number of length-depth combinations of potential defects that would all have failure pressures equal to the test pressure. Each successively deeper defect has to have a shorter length in order that they all have a common failure stress equal to the maximum stress level employed in the hydrostatic test. A satisfactory way to cover the theoretically infinite number of just-surviving defects is to choose nine defects ranging in depth between 10% and 90% of the wall thickness in 10% increments. It is assumed, and experience shows, that the calculated lives of defects that fall within a given 10% increment, at least for the worst-case defects, are very close to the lives calculated for the two defects on either end of the 10% increment. The fatigue crack growth software is used to calculate the numbers of cycles of applied pressure necessary to cause each of the nine just-barely-surviving defects to grow to a size that will cause it to fail at the maximum operating pressure (MOP). The operating pressure cycles for a representative period of operating time constitute a "block" or spectrum. The spectrum is applied repeatedly by the software until failure is predicted for each of the nine defects. The number of times the spectrum is applied is translatable into years of operation between the time of the test and the time of the failure. One of the nine defects usually has a shorter life than the other eight, and its time to failure controls the scheduling of a re-test.

When the objective of a fatigue analysis is to estimate the remaining life of defects that are found by an ILI crack-tool inspection, the specific dimensions of the identified defects (length and depth) are used as the initial defect sizes for starting the analysis. The number of repeated applications of the spectrum of pressure cycles needed to cause each defect to grow to failure gives the time to failure for that particular defect. That defect must be repaired or removed before the calculated time to failure has expired.

When the analysis is performed for the purpose of scheduling a future hydrostatic test, the location of any particular defect, if it exists, is unknown. Therefore, the analyst must take into account the hydraulic gradient and elevation changes along the pipeline and the variations in the test-pressure-to-operating-pressure ratio that occur as a result of the gradient and elevation changes in order to determine the worst-case time to failure. The worst-case time to failure may not always occur just outside the pump station of a segment, so multiple analyses at different locations may be needed to find the minimum time to failure. When the analysis is performed for the purpose of scheduling excavation and repair of particular (known) defects found by ILI,

the effective pressures at the location of each anomaly based on the location along the hydraulic gradient and elevation of the location should be used to calculate the times to failure.

Failure Criteria

The size of a defect, its length and depth, determine a unique value of failure pressure for a fixed set of pipe material properties and pipe geometry. Various models for calculating failure pressures exist such as the Modified LnSec model[iv], PAFFC[v], CorLas™[vi], and API 579, Level II[vii]. Typically, such a model is built into fatigue software to be used as needed. When a fatigue analysis is applied for the purpose of calculating a re-test interval for successive hydrostatic tests, the failure pressure model establishes the initial defect sizes based on the achieved test pressure. The failure pressure model is also employed periodically to recalculate the failure pressures of the "growing" defects and the fatigue analysis is terminated when the failure pressure of the worst-case defect decays to the MOP of the pipeline.

Pipeline Attributes

Regardless of which model is used to calculate failure pressures, the pipe geometry (diameter and wall thickness) and the key material properties (strength and toughness) must be known because the accuracy of the calculated failure pressures depends on these attributes. The diameter and wall thickness are generally known. However, if a pipeline is "telescoped," that is, built with segments of decreasing wall thickness based on the hydraulic gradient, the analyst must often analyze the remaining life for a location in each different wall thickness segment.

With respect to strength, the nominal yield strength and ultimate strength of the pipe material will generally be known, but the actual strengths of the individual pipes will not be known. For older pipeline systems, the toughness of the pipe material is often not known. Sometimes the pipeline operator may have Charpy V-notch upper-shelf energy levels for the pipe material. Charpy upper shelf energy can be used directly in most failure pressure prediction models as a surrogate for toughness. Fortunately, as will be shown by the sensitivity study presented herein, conservative estimates of fatigue life can be obtained by assuming suitable values of strength and toughness. Therefore, lack of knowledge about strength and toughness does not prevent the analyst from predicting satisfactory estimates of times to failure.

Pressure Cycles

A fatigue analysis should be based on pressure cycles that are truly representative of the operation of the pipeline being assessed. The only actual cycles available will be those taken from past operations. Quite often the pressure cycles over a recent one-year period will be representative because seasonal changes in demand will be taken into account. Of course, it is assumed that the future service conditions will not change from those of the chosen spectrum. If

it is expected that the demand will change significantly, the anticipated changes should be built into the pressure-cycle spectrum. An evolving technique involves continuous monitoring of cycles and using them to frequently update the analysis and the status of defects to project when the worst-case defect will grow large enough to fail at the MOP.

An important aspect of creating a representative spectrum of pressure cycles involves the sampling frequency. Changes in pressure on a hazardous liquid pipeline can occur very rapidly, so sampling the pressures at too long an interval could result in significant changes being missed. Generally, it is felt that the sampling interval should not exceed fifteen minutes, and minute-by-minute sampling or even 15-second sampling is not unusual. Large amounts of data can be generated if the sample interval is short, so a technique to reduce the data stored is to only capture changes in pressure that are above a certain threshold, typically 25 psig. Since only the changes in pressure are needed for the fatigue analysis, this method is optimal for ensuring that changes in pressure are captured while minimizing the data storage requirements.

Crack Growth Rates

The crack growth rate for a Paris-law type of analysis is characterized by the constants "*C*" and "*n*" in Equation 1. Equation 1 appears as a sloping straight line if plotted on a log-log plot as shown in Figure 1. The slope of the line is *n*, and its intercept is *C*. The relationship is linear over a range of ΔK values referred to as Region II. The straight line portion of Figure 1 has a slope of 3 and an intercept of 8.61E-19 for ΔK in psi$\sqrt{}$inch and da/dN in inch/cycle for a particular material and environment. The heavy dashed line extending downward from the straight-line portion represents Region I where the trend is that crack growth does not take place at a ΔK below a certain threshold value that may or may not be known. As illustrated by the upward-curving dashed line at high ΔK values, crack growth occurs by ever-larger stages of ductile tearing until failure takes place. The latter region is designated as Region III. The application of Equation 1, then, is strictly valid only throughout Region II.

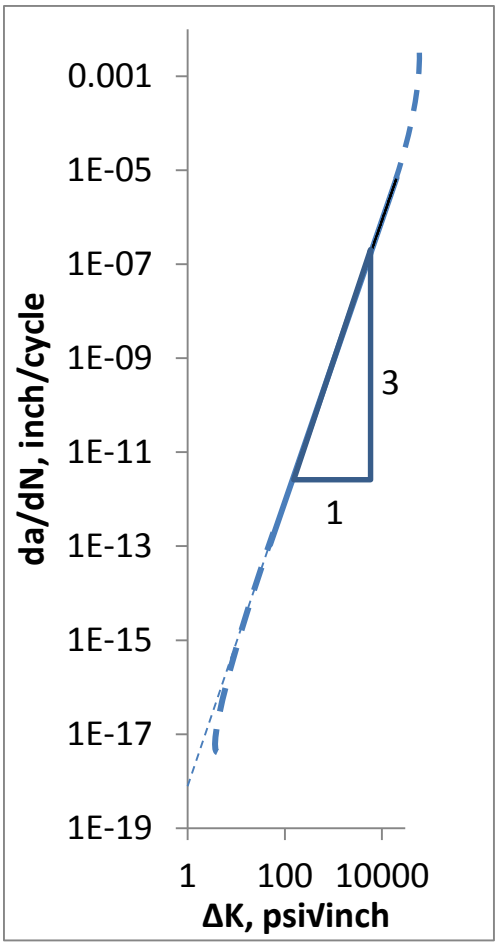

Figure 1. A Paris-Law Relationship for a Particular Material and Environment

Both the pipe material and the environment to which the material is exposed affect the crack growth rate constants. As will be shown in the sensitivity studies presented later in this document, the values of these constants have a significant influence on the time to failure of a defect. So, it is important for the analyst to choose either constants that accurately represent the material and the environment or constants that can be counted upon to produce conservative predictions of times to failure. The measurement of crack growth rates under actual service conditions is usually impractical. Therefore, most consultants rely on published values that have been generated by series of laboratory tests involving various materials in various environments. The particular set of constants illustrated in Figure 1 (C = 8.61E-19 and n = 3) are recommended in the API 579 document[viii] as default values for welded joints in structures comprised of ferritic steels (includes line pipe steels). A slightly less aggressive set of constants (C = 3.6E-19 and n = 3) is suggested in Reference 9 for ferritic steels in an air environment[ix].

SENSITIVITY STUDIES

Presented in this section of the document are calculations of times to failure for a hypothetical pipeline comprised of 16-inch-OD, 0.250-inch-wall, API 5L Grade X52 ERW line pipe. The maximum operating pressure (MOP) of this pipeline is 1,170 psig corresponding to a hoop stress level of 72% of SMYS. The pressure level corresponding to 100% of SMYS is 1,625 psig, and the pressure level corresponding to 90% of SMYS is 1,463 psig. The scenarios to be examined are:

- Times to failure for hypothetical defects that could barely survive a hydrostatic test
- Times to failure for specific defects identified as the result of an ILI crack-tool run

First, the factors that affect times to failure after a hydrostatic test are discussed. Then the factors that affect times to failure for anomalies found via ILI are discussed.

Times to Failure after a Hydrostatic Test

In these sensitivity studies of times to failure after a hydrostatic test we will examine the effects of:

- Material toughness
- Material flow stress
- Operational-pressure-cycle range
- Test-pressure-to-operating-pressure ratio
- Crack growth rate
- Pipe geometry

Times to failure after a hydrostatic test were calculated for 13 cases for defects that could have barely survived the test. HT Case 1 (meaning hydrostatic test Case 1 to distinguish it from ILI Case 1) is the baseline case. HT Case 1 involves the 16-inch-OD, 0.250-inch-wall, X52 material. The material was assumed to have a flow-stress of 62,000 psi (SMYS + 10,000 psi)[2] and a toughness corresponding to a full-size-equivalent Charpy upper-shelf energy of 20 ft lb[3]. For the baseline case it was assumed that the MOP of the pipeline was 1,170 psig and that the pipeline experiences one cycle of pressure ranging from zero to 1,170 psig and back to zero in a two-day period (182.5 full-range cycles per year). It was further assumed that the pipeline in the baseline

[2] A flow stress equal to SMYS+10,000 psi is a reasonable assumption for the base metal of a typical line pipe material manufactured prior to 1970.
[3] A Charpy energy of 20 ft lb would not be unusual for the base metal or ERW heat affected zone of a typical line pipe material manufactured prior to 1970.

case was tested to a pressure level of 1,625 psig corresponding to 100% of SMYS. Lastly, the crack growth rate constants were taken to be those given in the API 579 standard, namely, C = 8.61E-19 and n = 3. As seen in Table 1, certain parameters were changed from case to case to examine the effects of various factors that affect the predicted times to failure.

Table 1. Matrix of Hydrostatic Test Cases (yellow highlighted cells represent parameters that differed from the baseline case parameters)

	HT Case 1	HT Case 2	HT Case 3	HT Case 4	HT Case 5	HT Case 6	HT Case 7	HT Case 8	HT Case 9	HT Case 10	HT Case 11	HT Case 12	HT Case 13
Diameter, inches	16	16	16	16	16	16	16	16	16	16	30	8.625	16
Wall Thickness, inch	0.250	0.250	0.250	0.250	0.250	0.250	0.250	0.250	0.250	0.250	0.375	0.188	0.250
SMYS, psi	52,000	52,000	52,000	52,000	52,000	52,000	52,000	52,000	52,000	52,000	52,000	52,000	70,000
Maximum Operating Pressure, psig	1170	1170	1170	1000	1000	1170	1170	1170	1170	1170	936	1632	1575
Test Pressure, psig	1625	1625	1625	1625	1390	1463	1625	1625	1625	1625	1300	2267	2188
Test-pressure-to-operating-pressure	1.39	1.39	1.39	1.63	1.39	1.25	1.39	1.39	1.39	1.39	1.39	1.39	1.39
Minimum Pressure, psig	0	0	0	0	0	0	585	878	0	0	0	0	0
Pressure Cycle Range, psig	1170	1170	1170	1000	1000	1170	585	292	1170	1170	936	1632	1575
crack-growth rate intercept, C	8.61E-19	8.61E-19	8.61E-19	8.61E-19	8.61E-19	8.61E-19	8.61E-19	8.61E-19	8.61E-21	8.61E-19	8.61E-19	8.61E-19	8.61E-19
Crack-growth rate exponent, n	3	3	3	3	3	3	3	3	3	3.2	3	3	3
material toughness, CVN full-size-eq., ft lb	20	200	20	20	20	20	20	20	20	20	20	20	20
material flow stress, psig	62,000	62,000	82,000	62,000	62,000	62,000	62,000	62,000	62,000	62,000	62,000	62,000	80,000
Comparison parameter	baseline	high toughness	high flow stress	reduced MOP with same test pressure	reduced MOP with reduced test pressure	90% SMYS test	half range cycles	quarter range cycles	Smaller C	n=3.2	larger pipe	smaller pipe	higher grade

Times to Failure for the Baseline Case

The complete results of the fatigue analysis for HT Case 1 are shown in Figure 2. Presented in Figure 2 is a "results" page from the software PIPELIFE. It should be noted that other fatigue life software is available, and at least some of them are known to produce results similar to those of PIPELIFE. Not much full-scale pipe fatigue test data involving measuring the growth of cracks with continuing cyclic loading exist, but PIPELIFE was calibrated against three such tests conducted at Battelle[x].

Section 1. Analysis

Description:	Type 2
	baseline
	nominal properties

Section 2. Geometry

Diameter	16	
Wall Thickness	0.25	

Section 3. Material

Material	X52	
Yield Stress	52,000	
Flow Stress	62,000	psi
Charpy V-Notch	20	ft-lbs
Charpy V-Notch Area	0.124	sq-in
Young's Modulus (E)	30.0E+06	psi

Section 4. Pressure History

Max Operating Pressure	1,170	psig
Hydrostatic Test Pressure	1,625	psig
Max. Press. in Original Spectrum	1,170	psig
Min. Press. in Original Spectrum	0	psig
Amplitude Filter	25	psig
Max Operating Pressure	72%	%SMYS
Hydrostatic Test Pressure	100%	%SMYS
Max. Press. in Original Spectrum	72%	%SMYS

Section 5. Factors

Mean Shift Factor (Add)	0.0	
Scale Factor (Mult.)	1.000	
Crack Growth Rate Const. (C)	8.61E-19	
Crack Growth Rate Const. (n)	3	
Eccentricity (e/t)	0.01	

Section 6. Pressure History

Num. Pressure Histories	2	
# of Days Cycles Occurred	2	Days
Number of Cycles	1	
Conversion Factor *(Cycles/Year)*	182.6	

Section 7. Miscellaneous Input

Eccentricity	0.01	
Bending Multiplication Factor is	1.00	
Analysis Does Not Consider Threshold Effects		
Analysis Does Consider Bending Stress		

Section 8. Retest Interval and Safety Factor

Maximum Retest Interval	1.29	Years
Based on a Safety Factor of	2.000	

a/t Percent	a - Initial inch	c - Initial inch	Cycles to Failure	Years to Failure	a/t Final Percent	a - Final inch	c - Final inch	Pfail Defect Failure Press psig	Pmax in Failure Cycle psig
90.0%	0.2250	0.3400	543	3.0	96.3%	0.2408	0.3662	1,170	1,170
80.0%	0.2000	0.5200	478	2.6	92.6%	0.2315	0.5429	1,169	1,170
70.0%	0.1750	0.7000	472	2.6	88.3%	0.2209	0.7173	1,169	1,170
60.0%	0.1500	0.9050	509	2.8	83.4%	0.2084	0.9168	1,169	1,170
50.0%	0.1250	1.1750	586	3.2	77.2%	0.1929	1.1821	1,169	1,170
40.0%	0.1000	1.5550	777	4.3	69.8%	0.1745	1.5588	1,169	1,170
30.0%	0.0750	2.1650	1,311	7.2	60.9%	0.1522	2.1666	1,170	1,170
20.0%	0.0500	3.4500	2,883	15.8	48.8%	0.1220	3.4505	1,170	1,170
10.0%	0.0250	25.3900	7,656	41.9	27.9%	0.0698	25.3900	1,170	1,170

Figure 2. Results of Fatigue Analysis to Calculate Times to Failure after a Hydrostatic Test for HT Case 1

The input data for the case are included in Sections 1 through 8 on the "results" page, and the results of the calculations are shown at the bottom of the page for the nine representative defects

that could have barely survived the test. Section 1 documents a description of the case. "Type 2" means that the case was run for nine representative defects that could have barely survived the test. Sections 2 and 3 give the pipe geometry and material properties, respectively. Section 4 presents the operating pressure, the test pressure, the maximum and minimum pressures in the pressure-cycle-spectrum, and the limit on the amplitude of cycles that are counted (i.e, in this case cycles with amplitude below 25 psig are not counted.) The Effect of a 25-psig cycle on crack growth is insignificant when compared to the effect of a 1000-psig cycle. The ΔK value associated with a 25-psig cycle when raised to the power of "n" where n=3 is only 0.00156% of the ΔK associated with a 1000-psig cycle raised to the power of "n" where n=3.

Section 5 of the "results" page gives some key input parameters such as mean shift, scale factor, and eccentricity. The mean shift can be used to move the range of pressure cycles up or down in relationship to the maximum stress without changing the range. The scale factor can be used to change the range. A scale factor is sometimes used to look at the changing range of pressures along a hydraulic gradient or to evaluate hypothetical scenarios involving changes to the MOP. The eccentricity factor represents the amount of mismatch of the plate edges on either side of a seam. For all of the cases discussed herein these parameters were set at their default values (zero mean-shift, scale factor = 1, eccentricity = 0.01 inch). The default value of eccentricity in non-zero because it was found that the predictions were closer to actual test data when an eccentricity of 0.01 inch was used[xi]. The crack growth parameters used in the analysis, C and n, are also shown in Section 5.

Section 6 describes the pressure cycle spectrum. Section 7 presents miscellaneous parameters (inadvertently repeating eccentricity) that were not changed throughout these analyses. Section 8 gives the maximum retest interval based on a safety factor of 2. It is the minimum time to failure divided by 2. The appropriateness of a safety factor of 2 is discussed later in this document.

The listing of results for the 9 representative elliptically-shaped defects includes their depth-to-thickness ratios in percent, their actual depths in inches, and their half-lengths in inches. Next, the times to failure are given as "Cycles to Failure" and "Years to Failure". The remaining columns in the output give final depths and half-lengths at failure along with the final failure pressure.

In the HT Case 1 results it is seen that shortest predicted time to failure, 2.6 years, is associated with the defect that was initially 70% through the wall and had a full length of 1.4 inches (half-length of 0.7 inch). Usually the shortest life is associated with one of the deeper defects (60 to 80 percent through the wall) but seldom with the deepest defect (90 percent though the wall). This should not be surprising since the stress intensity factor range that drives crack growth is a

function of the absolute depth. That is clear from Equation 2, and therefore, one might expect the deepest defect to have the shortest life. However, there is another factor in play, and that is the fact that the stress intensity factors applicable at stress levels well below the failure stress are distributed differently around the peripheries of the 9 defects. To survive the test, a very-deep defect must also be very short. As a result, a very-short, very-deep defect may have to grow in length before it can grow fast in depth. Therefore, while rapid failure is expected for the deeper defects, the worst-case driving force may not always be associated with the deepest defect.

If HT Case 1 represented a real pipeline, the minimum predicted time to failure after a hydrostatic test, 2.6 years, would mean that the pipeline would have to be retested in 1.3 years if a factor of safety of 2 is applied to the calculated time to failure. As mentioned previously, the adequacy of a safety factor of 2 is discussed later in this document.

Effect of High Toughness

The effect of toughness as measured by Charpy upper-shelf energy (CVN) can be seen by comparing the results of HT Case 2 with those of HT Case 1. HT Case 2 was run with all parameters the same as those of HT Case 1 except that in Case 2 the CVN was assumed to be 200 ft lb instead of 20 ft lb as in HT Case 1. First, as one would expect with higher toughness, defects that survive the hydrostatic test are larger than those in a lower toughness pipe. This is seen in Table 2 in terms of the longer lengths for the higher-toughness material for a given a/t ratio.

Table 2. Effect of Toughness on Initial Defect Size (the compared variable is highlighted in yellow)

HT Case Number	CVN, ft lb	half length, c, inches for a/t ranging from 0.9 to 0.1								
		0.9	0.8	0.7	0.6	0.5	0.4	0.3	0.2	0.1
1	20	0.3400	0.5200	0.7000	0.9050	1.1750	1.5550	2.1650	3.4500	na
2	200	0.3400	0.5200	0.7000	0.9050	1.1800	1.5950	2.4600	7.5150	na

There is no difference for the deeper defects because they are relatively short. The influence of higher toughness shows up with longer defects (full lengths longer than about 2 inches or $\sqrt{Dt}$ for this pipe geometry). Note that due to built-in limitations in the software, the lengths calculated for a/t of 0.1 are not correct (denoted by "na" the table), but the trend is that the surviving defects in the 200-ft-lb material are larger than those of the 20-ft-lb material.

The effect on times to failure as shown in Table 3 is also what one would expect. The times to failure for the tougher material start to get shorter as the defects get longer (except for a/t = 0.1 because of the software limitation noted above). While it might seem counterintuitive that the times to failure would be shorter for the higher toughness material, the result comes about because of the larger starting defect sizes in the tougher material.

Table 3. Effect of Toughness on Times to Failure (the compared variable is highlighted in yellow)

HT Case Number	CVN, ft lb	Years to Failure for a/t ranging from 0.9 to 0.1								
		0.9	**0.8**	**0.7**	**0.6**	**0.5**	**0.4**	**0.3**	**0.2**	**0.1**
1	20	3.0	2.6	2.6	2.8	3.2	4.3	7.2	15.8	na
2	200	3.0	2.6	2.6	2.8	3.2	4.1	6.7	14.3	na

One might also wonder about the fact that higher toughness should also be expected to result in larger defects being necessary to cause failure at the MOP, and that such a circumstance might at least partially offset the effect of larger initial defect size. However, there is essentially no significant effect of increasing final defect size with increasing toughness. That is because the steps of defect growth become so large as the time of failure is approached, that the difference in time to failure is only a few cycles of pressure, not enough to register on the scale of a year or more in time.

An important conclusion that one can draw from this finding is that knowing the toughness of the material is important for calculating the time to failure after a hydrostatic test. However, the calculations also show that when the toughness is not known, one could make a conservative prediction of time to failure by simply assuming a very high value of toughness for determining the sizes of defects that could have barely survived the test.

Effect of High Flow Stress

The effect of flow stress can be seen by comparing the results of HT Case 3 with those of HT Case 1. HT Case 3 was run with all parameters the same as those of HT Case 1 except that in HT Case 3 the flow stress was assumed to be 82,000 psi instead of 62,000 psi as in HT Case 1. First, as one would expect with higher flow stress, defects that survive the hydrostatic test are larger than those in a material with a lower flow stress. This is seen in Table 4.

Table 4. Effect of Flow Stress on Initial Defect Size (the compared variable is highlighted in yellow)

HT Case Number	Flow Stress, psi	half length, c, inches for a/t ranging from 0.9 to 0.1								
		0.9	0.8	0.7	0.6	0.5	0.4	0.3	0.2	0.1
1	62,000	0.3400	0.5200	0.7000	0.9050	1.1750	1.5550	2.1650	3.4500	na
3	82,000	0.6050	0.9650	1.3400	1.7750	2.3400	3.3200	6.9350	na	na

The influence of higher flow stress is significant. For a given a/t ratio, the lengths are nearly double and in some cases more than double those associated with lower flow stress. Note that due to built-in limitations in the software, the lengths calculated for a/t of 0.1 (and, in one case for a/t of 0.2) are not given (denoted by "na" the table), but the trend is that the surviving defects in the material with a flow stress of 82,000 psi are much larger than those in the material with a flow stress of 62,000 psi.

The effect on times to failure is also significant as shown in Table 5. The times to failure for the material with a flow stress of 82,000 psi are much shorter than those for the material with a flow stress of 62,000 psi. While it might seem counterintuitive that the times to failure would be shorter for the higher strength material, the result comes about because of the larger starting defect sizes in the tougher material.

Table 5. Effect of Flow Stress on Times to Failure (the compared variable is highlighted in yellow)

HT Case Number	Flow Stress, psi	Years to Failure for a/t ranging from 0.9 to 0.1								
		0.9	0.8	0.7	0.6	0.5	0.4	0.3	0.2	0.1
1	62,000	3.0	2.6	2.6	2.8	3.2	4.3	7.2	15.8	na
3	82,000	0.8	0.8	0.8	0.9	1.3	2.2	4.5	na	na

One might also wonder about the fact that higher strength should also be expected to result in larger defects being necessary to cause failure at the MOP, and that such a circumstance might a least partially offset the effect of larger initial defect size. However, there is essentially no significant effect of increasing final defect size with increasing flow stress. That is because the steps of defect growth become so large as the time of failure is approached, that the difference in time to failure is only a few cycles of pressure, not enough to register on the scale of a year or more in time.

An important conclusion that one can draw from this finding is that knowing the flow stress of the material is important for calculating the time to failure after a hydrostatic test. However, the calculations also show that when the flow stress is not known, one could make a conservative prediction of time to failure by simply assuming a very high value of flow stress for determining the sizes of defects that could have barely survived the test.

Effect of Pressure Cycle Range

The effect of pressure cycle range can be seen in Table 6 and Table 7. The times to failure of HT Cases 4, 7, and 8 are compared to those of HT Case 1 in these tables. The input parameters of HT Cases 4, 7, and 8 involve pressure cycle spectra that differ from that of HT Case 1 and from those of each other. The maximum pressure for HT Case 4 was reduced from 1,170 psig to 1,000 psig forcing the pressure cycle range to be 1,000 psig instead of 1,170 psig as in HT Case 1. For HT Case 7 the MOP was still 1,170 psig, but the minimum pressure was set at 585 psig forcing the pressure cycle range to be 585 psig instead of 1,170 psig. For HT Case 8 the MOP was still 1,170 psig, but the minimum pressure was set at 878 psig forcing the pressure cycle range to be 293 psig instead of 1,170 psig. In all four cases the hydrostatic test pressure was held at 1,625 psig.

Table 6. Effect of Pressure Cycle Range on Initial Defect Size (the compared variable is highlighted in yellow)

HT Case Number	Range	Hydrostatic Test Pressure, psig	half length, c, inches for a/t ranging from 0.9 to 0.1								
			0.9	0.8	0.7	0.6	0.5	0.4	0.3	0.2	0.1
1	1170	1625	0.3400	0.5200	0.7000	0.9050	1.1750	1.5550	2.1650	3.4500	na
4	1000	1625	0.3400	0.5200	0.7000	0.9050	1.1750	1.5550	2.1650	3.4500	na
7	585	1625	0.3400	0.5200	0.7000	0.9050	1.1750	1.5550	2.1650	3.4500	na
8	293	1625	0.3400	0.5200	0.7000	0.9050	1.1750	1.5550	2.1650	3.4500	na

It is seen in Table 6 that the initial defect sizes do not vary with the pressure range. This is as one would expect because initial defect size is a function of pipe geometry, hydrostatic test pressure, flow stress, and toughness, none of which is affected by the applied pressure cycle size.

As seen in Table 7, however, the pressure range has a significant effect on the times to failure. The minimum time to failure in all four cases is determined by the 70%-through defect, and it is seen that those times are 2.6 years, 4.9 years 19.2 years, and 145 years, respectively, for HT Cases 1, 4, 7, and 8.

Table 7. Effect of Pressure Cycle Range on Times to Failure (the compared variable is highlighted in yellow)

HT Case Number	Range	Hydrostatic Test Pressure, psig	Years to Failure for a/t ranging from 0.9 to 0.1								
			0.9	0.8	0.7	0.6	0.5	0.4	0.3	0.2	0.1
1	1170	1625	3.0	2.6	2.6	2.8	3.2	4.3	7.2	15.8	na
4	1000	1625	5.6	4.9	4.9	5.2	5.9	7.6	12.5	27.1	na
7	585	1625	22.7	19.6	19.2	20.6	23.7	31.3	52.8	116.2	na
8	293	1625	175.7	150.5	146.5	156.6	179.1	236.8	398.9	876.9	2328.5

An assessment of these results is shown in Table 8.

Table 8. Assessment of the Effect of Pressure-Cycle Range on Times of Failure

HT Case Number	Pressure Cycle Range, psig	Ratios of Range Size	Times to Failure, years	Reciprocals of Ratios of Times To Failure	Range Size Ratios Raised to the n^{th} Power (where n=3)
1	1,170	1	2.6	1	1
4	1,000	0.85	4.9	0.53	0.61
7	585	0.50	19.2	0.14	0.125
8	293	0.25	145.0	0.018	0.016

The times to failure differ by much more than the ratios of the range sizes might suggest as can be seen by comparing "Ratios of Range Size" to "Reciprocals of Ratios of Times to Failure". The effect of range size raised to the 3rd power comes much closer to stating the effect of range size as can be seen by comparing the numbers in the last column of Table 8 to the numbers in the second last column. This is not a coincidence. It is a consequence of the Paris-law relationship as expressed in Equation 1 and the fact that the change in stress-intensity factor, ΔK, (which drives crack growth) is proportional to the cyclic stress range as expressed in Equation 2. Crack growth, da/dN, is proportional to ΔK raised to the n^{th} power, and n was assumed to be 3 for the material analyzed.

The effect of pressure cycle size also can be seen it terms of the relationships shown in Figure 3 along with another implication of the Paris-law relationship.

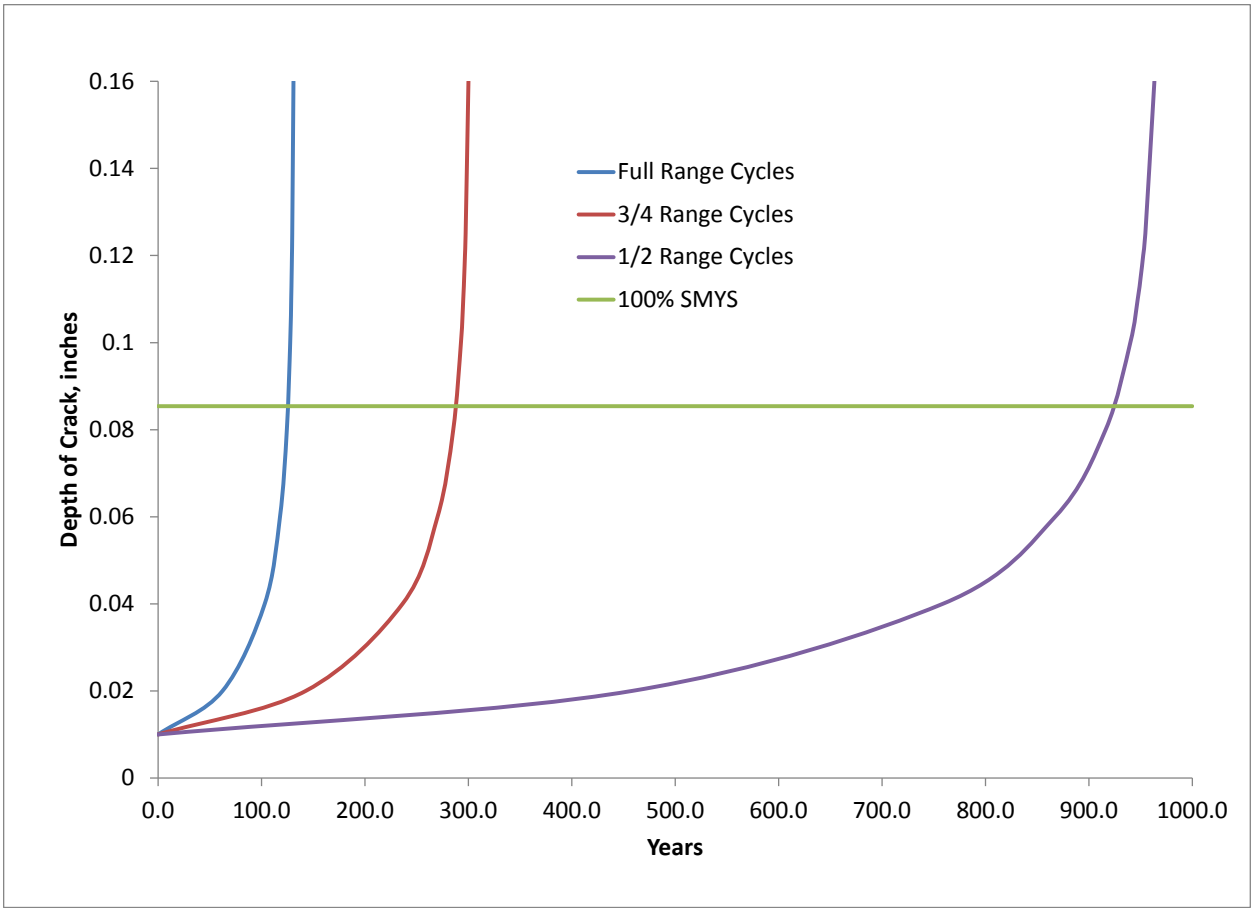

Figure 3. Effects of Pressure Cycle Size on Times to Failure for a 4-inch-long, 0.01-inch-deep defect in the Material Covered in HT Case 1

The three curves in this figure show crack-depth-versus-time-to-failure relationships for three ranges of pressure cycles for the 16-inch-OD, 0.250-inch, X52 material. One represents the case of full-range (zero to 72% of SMYS cycles), one represents the case of 3/4-range cycles (18 to 72% of SMYS), and one represents the case of half-range cycles (36 to 72% of SMYS). As can be seen, the times for a 4-inch-long, 0.01-inch-deep defect to grow to failure (where the curves become vertical) vary from about 130 years for the full-range cycles to about 300 years for the 3/4-range cycles to over 960 years for the 1/2-range cycles.

It is also apparent in Figure 3 that a 4-inch-long defect that could barely survive a hydrostatic test to 100% of SMYS is estimated to have a depth of 0.085 inch. Because of the shape of the depth-versus-time curve, the times to failure for the barely surviving defects are much shorter: 5.3 years with full-range cycles, 12.2 years with 3/4-range cycles, and 39 years with 1/2-range cycles. These much shorter lives for larger defects are a consequence of the fact that the stress intensity factor, ΔK, is a function of crack depth, a. As a increases even though stress range

remains constant, ΔK increases in proportion to $\sqrt{a}$. Hence, the rate of crack growth increases as the crack depth increases.

The effect of stress range on fatigue crack growth illustrates why failures involving fatigue crack growth are observed in hazardous liquid pipelines but have rarely been seen in natural gas pipelines. Natural gas pipelines typically are subject to much smaller ranges of stress than liquid pipelines normally are. This leads to the expectation that eventually, perhaps after hundreds of years of operation, failures from fatigue crack growth will appear in natural gas pipelines.

Effect of Test-Pressure-to-Operating-Pressure Ratio

The effect of test-pressure-to-operating-pressure ratio is illustrated by the comparisons involving HT Cases 1, 4, 5, and 6 in Table 9 and Table 10. The comparisons of interest in terms of test-pressure-to-operating-pressure ratio are between HT Cases 1 and 5, between HT Cases 1 and 6 and between HT Cases 4 and 5. The comparison between HT Case 1 and HT Case 4 was made previously in terms of the effect of stress range and is not considered again here because of the confounding effect of the two different stress ranges.

Table 9. Effect of Test-Pressure-to-Operating-Pressure Ratio on Initial Defect Size (the compared variable is highlighted in yellow)

HT Case Number	Range	Hydrostatic Test Pressure, psig	half length, c, inches for a/t ranging from 0.9 to 0.1								
			0.9	0.8	0.7	0.6	0.5	0.4	0.3	0.2	0.1
1	1170	1625	0.3400	0.5200	0.7000	0.9050	1.1750	1.5550	2.1650	3.4500	na
4	1000	1625	0.3400	0.5200	0.7000	0.9050	1.1750	1.5550	2.1650	3.4500	na
5	1000	1390	0.4950	0.7750	1.0800	1.4650	2.0150	2.8550	4.5250	16.6400	na
6	1170	1463	0.4450	0.6950	0.9550	1.2750	1.7150	2.3800	3.5600	8.1650	na

Table 10. Effect of Test-Pressure-to-Operating-Pressure Ratio on Times to Failure (the compared variable is highlighted in yellow)

HT Case Number	Range	Hydrostatic Test Pressure, psig	Years to Failure for a/t ranging from 0.9 to 0.1								
			0.9	0.8	0.7	0.6	0.5	0.4	0.3	0.2	0.1
1	1170	1625	3.0	2.6	2.6	2.8	3.2	4.3	7.2	15.8	na
4	1000	1625	5.6	4.9	4.9	5.2	5.9	7.6	12.5	27.1	na
5	1000	1390	1.9	1.9	1.9	2.0	2.5	4.0	8.4	20.6	na
6	1170	1463	1.2	1.1	1.2	1.3	1.6	2.5	5.1	11.9	na

First, consider the comparison between HT Case 1 and HT Case 5. Both cases have the same test-pressure-to-operating-pressure ratio, 1.39. Notice that the absolute value of test pressure is important because it establishes the remaining defect sizes. As shown in Table 9, the lower absolute value of test pressure in HT Case 5 means that larger defects must be assumed to exist than in HT Case 1. The result as shown in Table 10 is that even though the stress range associated with HT Case 5 is less than that associated with HT Case 1, the times to failure for HT Case 5 are shorter than those for HT Case 1. Now consider the result of HT Case 4 which has the same operating stress range as that of HT Case 5 but a higher test-pressure-to-operating-pressure ratio (1.625). The higher test pressure in HT Case 4 assures the presence of smaller remaining defects as shown in Table 9. Consequently, as shown in Table 10, the times to failure for HT Case 4 are longer than those for HT Case 5 even though the stress range is the same in both cases.

Next, consider the comparison between HT Case 1 and HT Case 6. Both have the same operating stress range. The pipe in HT Case 1 is tested to a level of 100% of SMYS corresponding to a test-pressure-to-operating-pressure ratio of 1.39. The pipe in HT Case 6 is tested to a level of 90% of SMYS. The remaining defects associated with HT Case 6 are larger than those associated with HT Case 1, and, correspondingly, the times to failure for HT Case 6 are significantly shorter than those associated with HT Case 1.

The concepts embodied in these comparisons can also be seen in terms of Figure 4.

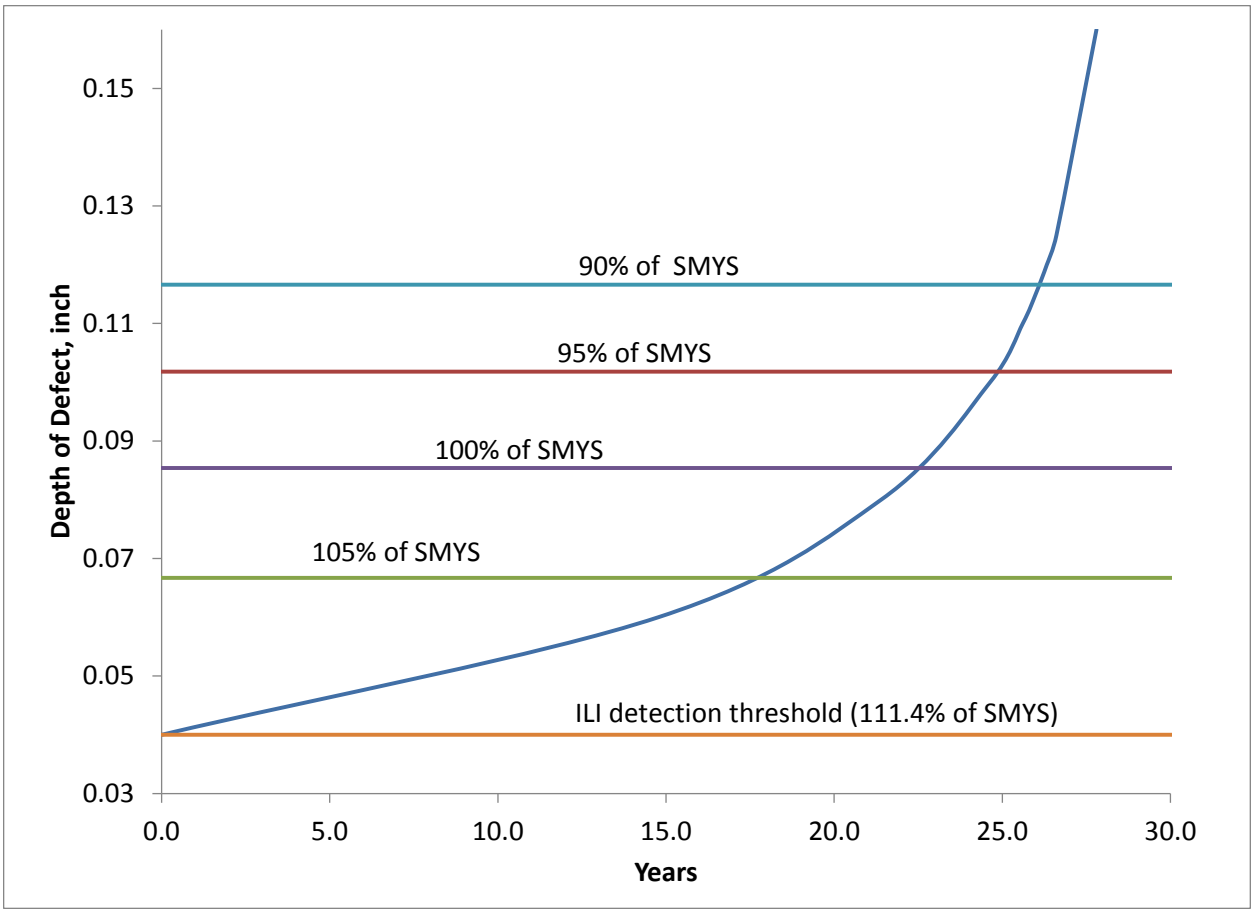

Figure 4. Effect of Test-Pressure-to-Operating-Pressure Ratio on Times to Failure for a 4-inch-long Defect in a Pipeline that is Operated at 72% of SMYS

This figure shows an expanded-time-scale view of the end of the full-range-cycle depth-versus-years curve shown in Figure 3. Recall that this involves a 16-inch-OD, 0.250-inch wall, X52 pipeline that is operated at 72% of SMYS and is subjected to one full-range cycle (0 to 72% of SMYS and back to 0) every 2 days. At Year Zero on Figure 4, the defect has a depth to 0.040 inch, and it is predicted to fail at a hoop stress level of 111.4% of SMYS. In 27.8 years it will grow to a depth of 0.160 inch, and at that depth it would fail at a stress level of 72% of SMYS.

The horizontal lines as various depths represent various stress levels that would cause the defect to fail at a particular time after Year Zero. The points where these lines intersect the depth-versus-time curve indicate the number of years from Year Zero that are required for the defect to attain the depth that would lower its failure stress to the particular test stress level. So, one can find the remaining time to failure from each intersection point by subtracting the years to that point from 27.8 years (the time at which the defect becomes deep enough to fail at 72% of SMYS). The results are summarized in Table 11.

Table 11. Times to Failure for Various Test Scenarios

Stress Level that Defect Barely Survives, %SMYS	Test-Pressure-to-Operating – Pressure Ratio	Depth of Defect, inch	Years for Defect to Grow to Failure
90	1.25	0.1166	1.6
95	1.32	0.1018	2.9
100	1.39	0.0854	5.3
105	1.46	0.0667	10.2
111.4	1.55	0.0400	27.8

The times to failure after a test of a particular level based on the data in Table 11 are shown in Figure 5.

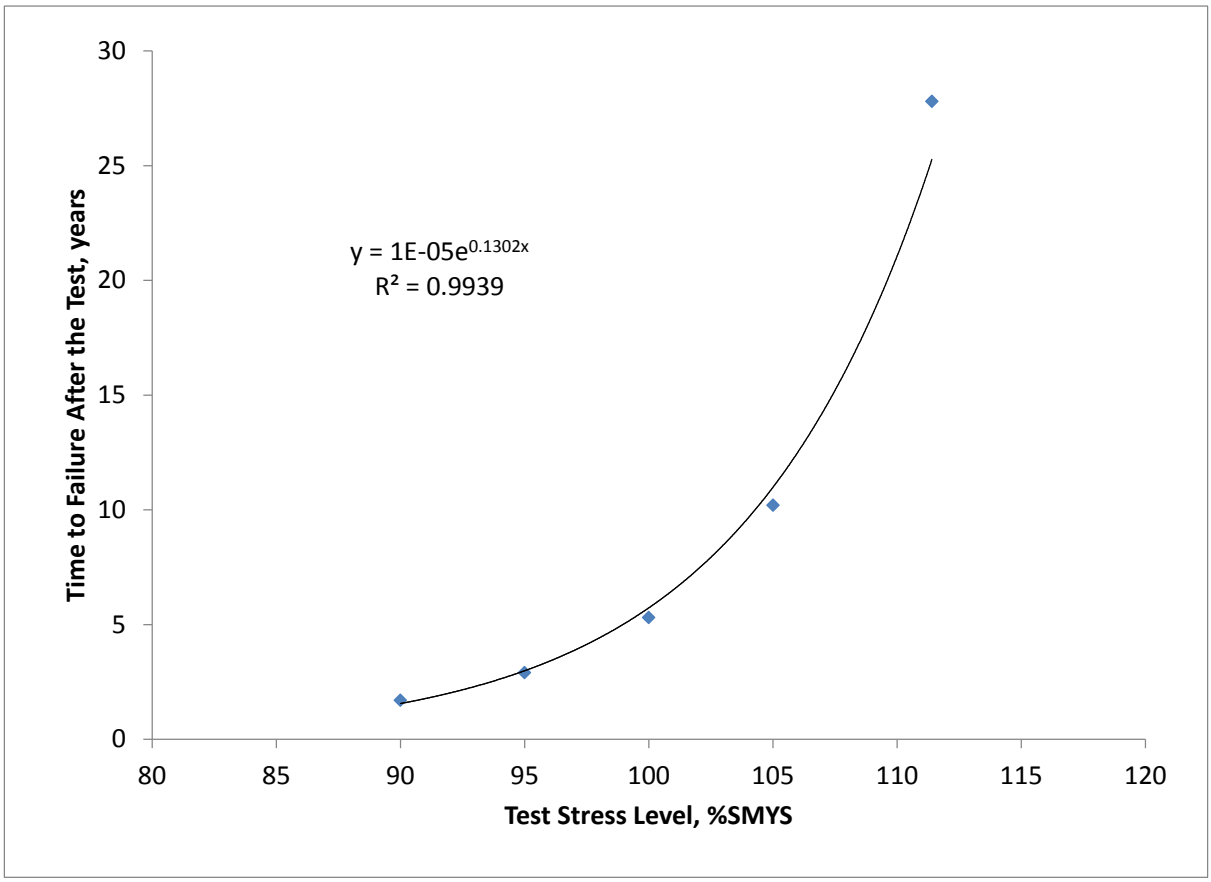

Figure 5. Relationship between Time to Failure and Test Pressure

As seen in Figure 5, the times to failure increase at an exponential rate with increasing test pressure. So, using the highest feasible test pressure assures a longer interval before a retest is needed. One practical upper limit on test pressure is that the test pressure should not be so high

that significant plastic expansion of the pipe begins to occur. Another practical upper limit is that the number of test failures may become intolerable in terms of the time the pipeline will be out of service. It is noted that the test pressure level of 111.4 % of SMYS is likely not feasible for both of these reasons. However, that level does correspond to the depth of a 4-inch-long defect that would be deep enough (0.040-inch) to be detected by a reliable ILI crack-detection tool. This illustrates a very significant advantage to using a reliable ILI tool for ERW seam integrity assessment instead of a hydrostatic test. The use of the ILI tool followed by the remediation of certain defects could make possible much longer re-assessment intervals than would be possible with hydrostatic testing within practical test stress limits.

The relationship between Time to Failure and Test Pressure illustrates three important points. One is that for a given pipeline, the higher the test-pressure-to-operating-pressure is, the longer the times to failure will be. The other point is that for pipelines that operate at a lower stress level, a given test-pressure-to-operating-pressure ratio will not be as effective as it would be in a pipeline operated at a higher stress level. This is because the remaining defect size becomes smaller as the test stress becomes closer to the flow stress of the material. For pipelines that are operated at lower stress levels (e.g., well below 72% of SMYS), the operator should consider utilizing a test-pressure-to-operating-pressure ratio greater than 1.39 and certainly one greater than 1.25. This is illustrated by the comparison of HT Case 4 and HT Case 5 in Table 10 both of which have a maximum operating stress of 61.5% of SMYS. The only difference between these cases is that HT Case 4 involved a test to100% of SMYS (a test-pressure-to-operating-pressure ratio of 1.625) whereas HT Case 5 involved a test to 85.5% of SMYS (a test-pressure-to-operating-pressure ratio of 1.39). The minimum predicted time to failure for HT Case 4 was more than 2.5 times the minimum predicted time to failure for HT Case 5.

Lastly, the intervals between ERW seam integrity assessments could be significantly longer with the use of a reliable ILI crack-detection tool than the intervals likely to be achieved via hydrostatic testing.

Effects of Crack Growth Rate Parameters

The effects of crack growth rate parameters (C and n in Equation 1) are illustrated by comparisons between HT Case 1 and HT Case 9, and between HT Case 1 and HT Case 10. The results of these comparisons are presented in Table 12 and Table 13.

Table 12. Effects of Changes in Crack Growth Parameters on Initial Defect Size (the compared variable is highlighted in yellow)

HT Case Number	C	n	half length, c, inches for a/t ranging from 0.9 to 0.1								
			0.9	0.8	0.7	0.6	0.5	0.4	0.3	0.2	0.1
1	8.61E-19	3	0.3400	0.5200	0.7000	0.9050	1.1750	1.5550	2.1650	3.4500	na
9	8.61E-21	3	0.3400	0.5200	0.7000	0.9050	1.1750	1.5550	2.1650	3.4500	na
10	8.61E-19	3.2	0.3400	0.5200	0.7000	0.9050	1.1750	1.5550	2.1650	3.4500	na

Table 13. Effects of Changes in Crack Growth Parameters on Times to Failure (the compared variable is highlighted in yellow)

HT Case Number	C	n	Years to Failure for a/t ranging from 0.9 to 0.1								
			0.9	0.8	0.7	0.6	0.5	0.4	0.3	0.2	0.1
1	8.61E-19	3	3.0	2.6	2.6	2.8	3.2	4.3	7.2	15.8	na
9	8.61E-21	3	297.0	260.9	257.7	278.2	320.0	424.8	717.0	1577.9	na
10	8.61E-19	3.2	0.4	0.3	0.3	0.3	0.4	0.5	0.9	2.0	na

Notice that the initial defect sizes are the same for all three cases in Table 12. That is because the initial defect sizes are determined solely by pipe geometry, toughness, flow stress, and hydrostatic test pressure. Changes in the crack growth parameters have no effect on the initial defect sizes.

The comparison between HT Case 1 and HT Case 9 is based on two different values of the parameter *C*. The two *C* values differ by two orders of magnitude. It is seen in Table 13 that the times to failure also differ by two orders of magnitude. This result is a direct consequence of the Paris-law relationship as expressed in Equation 1. The *C* value is a constant. When Equation 1 is reconfigured to integrate *dN* to get the number of cycles to failure, *C* is not altered by the integration. The answer in terms of cycles is proportional to *C*. If *C* changes by two orders of magnitude, so does the time to failure.

The comparison between HT Case 1 and HT Case 10 is based on two different values of the parameter *n*. For HT Case 1, *n* is equal to 3. For HT Case 10, *n* is equal to 3.2. As shown in Table 13, the times to failure associated with the higher *n* value of 3.2 are significantly shorter (by nearly an order of magnitude) than those associated with the *n* value of 3 even though the *n* values only differ by 7 percent. This result is a consequence of the Paris-law relationship as expressed in Equation 1. The stress intensity factor, ΔK, is raised to the power *n*. Thus $\Delta K^{3.2}$ is 1.58 times ΔK^3 for a ΔK of 10 ksi$\sqrt{inch}$ and 1.82 times ΔK^3 for a ΔK of 20 ksi$\sqrt{inch}$ not accounting for the fact that *a* would be increasing at a faster rate because *da/dN* is enlarged by

these factors. Therefore, the fact that a small change in *n* can lead to large changed in predicted times to failure is not surprising.

The comparisons of the effects of the crack growth parameters show that the parameters have a significant influence on predicted times to failure. Unfortunately, it is not easy to evaluate the crack growth parameters for a particular pipeline and its environment. Experience has shown that the values embodied in the API 579 document (C = 8.61E-19 for ΔK in psi$\sqrt{inch}$ and *da/dN* in inches/cycle and *n* = 3) provide adequately conservative values of these parameters.

Effect of Pipe Geometry

The effect of pipe geometry is shown in Table 14 and Table 15. These comparisons show that the diameter and wall thickness have an influence on predicted times to failure. Although it is not immediately apparent from these comparisons, the predicted fatigue life is inversely proportional to the ratio of diameter to wall thickness when all other parameters are equal (i.e. equivalent flow stress, MOP as percent of SMYS, and test-pressure-to-operating pressure ratio). Therefore, larger diameter, thinner wall pipe (i.e. high D/t ratio) would have shorter predicted times to failure than smaller diameter pipe of the same wall thickness. Furthermore, for pipes having different diameters and wall thicknesses but the same D/t ratio, the predicted fatigue life is inversely proportional with the diameter.

Table 14. Effects of Changes in Pipe Geometry on Initial Defect Size (the compared variable is highlighted in yellow)

HT Case Number	Diameter, inches	Wall Thickness, inch	MOP, psig	Hydrostatic Test Pressure, psig	half length, c, inches for a/t ranging from 0.9 to 0.1								
					0.9	0.8	0.7	0.6	0.5	0.4	0.3	0.2	0.1
1	16	0.250	1,170	1,625	0.3400	0.5200	0.7000	0.9050	1.1750	1.5550	2.1650	3.4500	na
11	30	0.375	936	1,300	0.5700	0.8700	1.1650	1.4950	1.8800	2.3500	3.0250	4.4950	na
12	8.625	0.188	1,632	2,267	0.2200	0.3300	0.4450	0.5800	0.7500	1.0150	1.5200	2.7500	na

Table 15. Effects of Changes in Changes in Pipe Geometry on Times to Failure (the compared variable is highlighted in yellow)

HT Case Number	Diameter, inches	Wall Thickness, inch	MOP, psig	Hydrostatic Test Pressure, psig	Years to Failure for a/t ranging from 0.9 to 0.1								
					0.9	0.8	0.7	0.6	0.5	0.4	0.3	0.2	0.1
1	16	0.250	1,170	1,625	3.0	2.6	2.6	2.8	3.2	4.3	7.2	15.8	na
11	30	0.375	936	1,300	2.0	1.8	1.8	2.0	2.5	3.5	6.2	13.3	na
12	8.625	0.188	1,632	2,267	4.4	4.0	3.8	3.9	4.4	5.5	8.4	17.8	na

Effect of Pipe Grade

The effect of pipe grade is shown in Table 16 and Table 17. These comparisons are presented to illustrate that pipe grade is important, but no significant point about the methodology can be derived from the comparison.

Table 16. Effects of Changes in Pipe Grade on Initial Defect Size (the compared variable is highlighted in yellow)

HT Case Number	SMYS, psi	MOP, psig	Hydrostatic Test Pressure, psig	half length, c, inches for a/t ranging from 0.9 to 0.1								
				0.9	0.8	0.7	0.6	0.5	0.4	0.3	0.2	0.1
1	52,000	1,170	1,625	0.3400	0.5200	0.7000	0.9050	1.1750	1.5550	2.1650	3.4500	na
13	70,000	1,575	2,188	0.2900	0.4450	0.5900	0.7550	0.9450	1.1750	1.4900	2.0600	5.2750

Table 17. Effects of Changes in Pipe Grade on Times to Failure (the compared variable is highlighted in yellow)

HT Case Number	SMYS, psi	MOP, psig	Hydrostatic Test Pressure, psig	Years to Failure for a/t ranging from 0.9 to 0.1								
				0.9	0.8	0.7	0.6	0.5	0.4	0.3	0.2	0.1
1	52,000	1,170	1,625	3.0	2.6	2.6	2.8	3.2	4.3	7.2	15.8	na
13	70,000	1,575	2,188	1.8	1.5	1.5	1.5	1.8	2.4	3.7	7.4	18.5

Conclusions Regarding the Effects of Various Fatigue Analysis Parameters on Predicted Times to Failure after a Hydrostatic Test

On the basis of the sensitivity study of parameters that affect the calculated times to failure after a hydrostatic test, the following conclusions may be drawn. Particular attention should be focused on Conclusions 3 and 4 as these points may at first seem counter-intuitive. Both points are relevant to making conservative predictions of times to failure after a hydrostatic test.

1. Times to failure after a hydrostatic test that could result from fatigue crack growth can be estimated using a "Paris-law" approach, provided that the user is able to supply the relevant data that includes, pipe geometry and strength level, the relevant operating pressure-cycle spectrum and test pressure history for the segment being assessed. Factors such as material toughness and flow stress can be addressed in the absence of actual data by using conservative assumptions. Satisfactory crack growth rate constants for the analysis can be found in the API 579 standard for fitness-for-service.

2. In using fatigue analysis to calculate the time to failure after a hydrostatic test, it must be assumed that defects could exist anywhere along the pipeline that are severe enough to have failure pressures no higher than that of the hydrostatic test pressure.

3. For a pipeline where the effective toughness of the ERW seam region is unknown, it is appropriate to assume a high value of toughness because the higher the toughness used in the analysis is, the shorter will be the predicted times to failure after the test. For the particular analysis method used herein, a toughness level corresponding to a full-size-equivalent Charpy upper shelf energy level of 200 ft lb was an appropriate value.

4. For a pipeline where the effective flow stress of the ERW seam region is unknown, it is appropriate to assume a high value of flow stress because the higher the flow stress used in the analysis is, the shorter will be the predicted times to failure after the test. Because ERW pipe materials are required to have a transverse strength level that exceeds that specified minimum ultimate tensile strength of the base metal, it is appropriate to assume a flow stress level at least as high as the specified minimum ultimate tensile strength of the base metal. In the case of older Grade B materials or early X-grade materials (made prior to 1949 by agreement between the manufacturer and the purchaser), it is probably prudent to add another 10,000 psi to the specified minimum ultimate tensile strength, as these materials often were much stronger than implied by the specified minimum strength parameters.

5. The calculated times to failure are strongly dependent on the actual pressure cycle spectrum to which a particular location on a pipeline is subjected. To calculate the minimum time to failure, more than one location along a pipeline may have to be examined because of elevation differences, hydraulic gradients, and/or wall thickness changes.

6. The calculated time to failure after a hydrostatic test increases exponentially with increasing test-pressure-to-operating-pressure ratio.

7. For a pipeline that is operated at maximum stress levels below 72% of SMYS, the test-pressure-to-operating-pressure ratio must be greater than that applied on a pipeline that operates at 72% of SMYS to achieve the same time to failure as that for the pipeline that operates at 72% of SMYS.

8. The time to failure after a hydrostatic test is strongly dependent on the crack growth rate constants employed in the Paris-law equation. Since the actual constants that apply in a

particular situation are usually unknown, the constants given in API Standard 579 may be used. Experience suggests that those constants are sufficiently conservative.

9. Assessment of ERW seam integrity using a reliable ILI crack-detection tool should permit longer intervals between re-assessments than is the case with repeated hydrostatic testing because an ILI tool should be able to find much smaller defects than those that can survive a hydrostatic test to the highest feasible test stress levels.

Times to Failure after an ILI Crack-Tool Run

Assessment of ERW seam integrity using a reliable ILI crack-detection tool results in the identification of anomalies by their locations and by their lengths and depths. The failure stress levels of the identified anomalies can be calculated based on the dimensions of the anomalies, the pipe geometry, and the toughness and flow stress of the pipe material. As a result one can prioritize the anomalies by decreasing failure stress for the purpose of examining them in the field and repairing those that need repairing. For those that are judged to have failure stresses sufficiently high to justify not examining them, fatigue analysis can be used to assess the times for them to grow to failure. Unlike in the case of fatigue analysis after a hydrostatic test, a fatigue analysis after an ILI tool run deals with specific listed dimensions for each remaining anomaly.

In these sensitivity studies of times to failure after an ILI crack-tool-run we will examine the effects of:

- Material toughness
- Material flow stress
- Potential depth sizing errors
- Potential length sizing errors

It is not necessary to examine the effects of pressure-cycle range, pipe geometry, pipe-material grade, or crack growth rate constants because the effects of these parameters are the same whether starting with a family of defects that survive a test or with a single defect based on ILI-provided dimensions.

Times to failure after a hypothetical ILI crack-tool run were calculated for 15 cases. ILI Case 1, the baseline case, involved the 16-inch-OD, 0.250-inch-wall, X52 material, the same as that used in HT Case 1, the baseline case for times to failure after a hydrostatic test. The material was

assumed to have a flow-stress of 62,000 psi (SMYS + 10,000 psi)[4] and a toughness corresponding to a full-size-equivalent Charpy upper-shelf energy of 20 ft lb[5]. For the baseline case it was assumed that the MOP of the pipeline was 1170 psig and that the pipeline experiences one cycle of pressure ranging from zero to 1170 psig and back to zero in a two-day period (182.5 full-range cycles per year). Lastly, the crack growth rate constants were taken to be those given in the API 579 standard, namely, C = 8.61E-19 and n = 3. Because each analysis addresses a specific defect rather than a family of defects that could have survived a particular hydrostatic test stress level, the depth and half-length of each initial defect are specified. For the baseline case the half-length of the defect was assumed to be 0.7 inch and its depth was assumed to be 0.175 inch, the same dimensions of as those of the defect that gave the shortest time to failure in HT Case 1. The pressure level of any past hydrostatic test is ignored in this type of analysis (i.e., when the initial dimensions are specified) even if the defect would have failed in a previous hydrostatic test.

As seen in Table 18, certain parameters were changed from case to case to examine the effects of various factors that affect the predicted times to failure.

[4] A flow stress equal to SMYS+10,000 psi is a reasonable assumption for the base metal of a typical line pipe material manufactured prior to 1970.
[5] A Charpy energy of 20 ft lb would not be unusual for the base metal or ERW heat affected zone of a typical line pipe material manufactured prior to 1970.

Table 18. Matrix of ILI Cases (yellow highlighted cells represent parameters that differed from the baseline case)

	ILI Case 1	ILI Case 2	ILI Case 3	ILI Case 4	ILI Case 5	ILI Case 6	ILI Case 7	ILI Case 8	ILI Case 9	ILI Case 10	ILI Case 11	ILI Case 12	ILI Case 13	ILI Case 14	ILI Case 15
crack depth, inch	0.175	0.150	0.125	0.100	0.105	0.060	0.040	0.040	0.040	0.066	0.070	0.193	0.116	0.175	0.060
crack length, inches	1.4	1.4	1.4	1.4	2.8	5.5	8	8	8	5.5	5.5	1.4	2.8	1.75	6.875
half crack length, inches	0.70	0.70	0.70	0.70	1.40	2.75	4.00	4.00	4.00	2.75	2.75	0.70	1.40	0.88	3.44
failure pressure, psig	1623	1723	1789	1836	1641	1627	1656	2122	1733	1596	1574	1516	1596	1509	1,565
failure stress, SMYS	99.9	106.0	110.1	113.0	101.0	100.1	101.9	130.6	106.7	98.2	96.9	93.3	98.2	92.9	96.3
material toughness, CVN	20	20	20	20	20	20	20	20	200	20	20	20	20	20	20
material flow stress, psig	62,000	62,000	62,000	62,000	62,000	62,000	62,000	82,000	62,000	62,000	62,000	62,000	62,000	62,000	62,000
Time to failure, years	2.6	4.4	7.0	11.0	4.2	11.2	23.8	25.8	24.4	8.8	7.5	1.5	3.1	1.5	7.2
Cycles to failure	472	813	1,284	2,005	768	2,055	4,341	4,720	4,449	1,610	1,368	278	570	276	1,312
Comparison Parameter	Base-line	depth	depth	depth	depth and length	depth and length	depth and length	high flow stress	high tough-ness	10% depth error, shallow	17% depth error, shallow	10% depth error, deep	10% depth error, mediu m	25% length error, short	25% length error, long

The following parameters were the same for all of the cases listed in Table 18.

- Diameter 16 inches
- Wall thickness 0.250 inch
- Grade X52
- MOP 1170 psig
- Pressure Cycle 0 to 1170 to 0 every 2 days
- C 8.61E-19 for ΔK in psi$\sqrt{inch}$ and da/dN in inches/cycle
- n 3

Time to Failure for the Baseline Case

The complete results of the fatigue analysis for ILI Case 1 are shown in Figure 6. Presented in Figure 6 is a "results" page from the software PIPELIFE.

Section 1. Analysis

Description:	Type 1
	baseline
	nominal properties

Section 2. Geometry

Diameter	16	
Wall Thickness	0.25	

Section 3. Material

Material	X52	
Yield Stress	52,000	
Flow Stress	62,000	psi
Charpy V-Notch	20	ft-lbs
Charpy V-Notch Area	0.124	sq-in
Young's Modulus (E)	30.0E+06	psi

Section 4. Pressure History

Max Operating Pressure	1,170	psig
Hydrostatic Test Pressure	1,625	psig
Max. Press. in Original Spectrum	1,170	psig
Min. Press. in Original Spectrum	0	psig
Amplitude Filter	25	psig
Max Operating Pressure	72%	%SMYS
Hydrostatic Test Pressure	100%	%SMYS
Max. Press. in Original Spectrum	72%	%SMYS

Section 5. Factors

Mean Shift Factor (Add)	0.0	
Scale Factor (Mult.)	1.000	
Crack Growth Rate Const. (C)	8.61E-19	
Crack Growth Rate Const. (n)	3	
Eccentricity (e/t)	0.01	

Section 6. Pressure History

Num. Pressure Histories	2	
# of Days Cycles Occurred	2	Days
Number of Cycles	1	
Conversion Factor *(Cycles/Year)*	182.6	

Section 7. Miscellaneous Input

Eccentricity	0.01	
Bending Multiplication Factor is	1.00	
Analysis Does Not Consider Threshold Effects		
Analysis Does Consider Bending Stress		

Section 8. Retest Interval and Safety Factor

Maximum Retest Interval	1.29	Years
Based on a Safety Factor of	2.000	

a/t Percent	a - Initial inch	c - Initial inch	Cycles to Failure	Years to Failure	a/t Final Percent	a - Final inch	c - Final inch	Pfail Defect Failure Press psig	Pmax in Failure Cycle psig
70.0%	0.1750	0.7000	472	2.6	88.3%	0.2209	0.7173		

Figure 6. Results of Fatigue Analysis to Calculate Times to Failure after an ILI Crack-tool Inspection for ILI Case 1

The input data for the case are included in Sections 1 through 8 on the "results" page, and the results of the calculation are shown at the bottom of the page for a single specific defect with a fixed depth, *a*, and a fixed half-length, *c*. "Type 1" means that the case was run for a single specific defect. A Type 1 analysis can be conducted for each anomaly in a list of anomalies provided by the ILI service provider. Sections 2 through 8 present the same information that was explained in conjunction with Figure 2. The information includes pipe geometry and material properties, operating pressure, the test pressure, the maximum and minimum pressures in the pressure-cycle-spectrum, and the limit on amplitude of cycles that are counted, mean shift, scale factor, eccentricity, the crack growth parameters used in the analysis (*C* and *n*), the pressure cycle spectrum, miscellaneous parameters, and the maximum retest interval based on a safety factor of 2. It is noted that test pressure is listed here, but it is not used in a Type 1 analysis.

Instead the cycles to failure for a specific defect are calculated. That specific defect will have a unique (and predictable) failure pressure that may be less than, equal to, or greater than the pressure employed in the most recent hydrostatic test of the pipeline.

The result at the bottom is given for the specific elliptically-shaped defect with a depth, *a*, and a half-length, *c*. The time to failure is given as "Cycles to Failure" and "Years to Failure". The remaining columns in the output give the final depth and half-length at failure.

In the ILI Case 1 results it is seen that shortest predicted time to failure is 2.6 years and that the specific defect was initially 70% through the wall and had a full length of 1.4 inches (half-length of 0.7 inch). Note that this defect is identical to the one that was predicted to have the shortest time to failure after a hydrostatic test to 1625 psig in the HT Case 1 hydrostatic test. The specific defect for ILI Case 1 was chosen for that reason.

If ILI Case 1 represented a real pipeline, the predicted time to failure for the specific defect would be 2.6 years, and it would mean that the defect would have to be excavated and examined in 1.3 years if a factor of safety of 2 is applied to the calculated time to failure. As mentioned previously, the adequacy of a safety factor of 2 is discussed later in this document.

Examining Anomalies with Various Depths and Lengths Based on Times to Failure

The results of an ILI run will contain a listing of anomalies that gives their lengths and depths as well as their location along the pipeline. ILI Cases 1 through 7 were created to show how such a list might look and to compare the times to failure based on fatigue analysis. The comparisons are shown in Table 19.

Table 19. Comparisons of Failure Stresses and Times to Failure for a List of Anomalies from a Hypothetical ILI Crack-tool Run

ILI Case Number	Crack Depth, inch	Crack Length, inches	Half Length, inches	Predicted Failure Pressure, psig	Predicted Failure Stress, %SMYS	CVN, ft lb	Flow Stress, psi	Time to Failure, years	Cycles to Failure
1	0.175	1.4	0.70	1,623	99.9	20	62,000	2.6	472
2	0.150	1.4	0.70	1,723	106.0	20	62,000	4.4	813
3	0.125	1.4	0.70	1,789	110.1	20	62,000	7.0	1,284
4	0.100	1.4	0.70	1,836	113.0	20	62,000	11.0	2,005
5	0.105	2.8	1.40	1,641	101.0	20	62,000	4.2	768
6	0.060	5.5	2.75	1,627	100.1	20	62,000	11.2	2,055
7	0.040	8	4.00	1,656	101.9	20	62,000	23.8	4,341

The failure stress levels, except for the ILI Case 1, exceed 100% of SMYS, so the operator of the pipeline might decide not to examine these anomalies immediately and wait for a period of time based on the predicted times to failure to examine them. If a factor of safety of 2 on time to failure is employed, the operator would want to examine each of these anomalies by the time half of the time to failure has expired. On this basis the time limit for examining the ILI Case 1 anomaly would be 1.3 years. Similarly, the other anomalies could be examined at times ranging from 2.1 to 11.9 years.

Effect of High Flow Stress

The effect of high flow stress is examined by comparing ILI Cases 7 and 8 in Table 20.

Table 20. Effect of High Flow Stress on Time to Failure after an ILI Run (the compared parameter is highlighted in yellow)

ILI Case Number	Crack Depth, inch	Crack Length, inches	Half Length, inches	Predicted Failure Pressure, psig	Predicted Failure Stress, %SMYS	CVN, ft lb	Flow Stress, psi	Time to Failure, years	Cycles to Failure
7	0.040	8	4.00	1,656	101.9	20	62,000	23.8	4,341
8	0.040	8	4.00	2,122	130.6	20	82,000	25.8	4,720

It is seen in Table 20 that the case involving the higher flow stress has a longer time to failure than the one involving the lower flow stress. This outcome differs from the effect of flow stress on time to failure after a hydrostatic test that was shown previously in Table 5. In that case the higher flow stress led to a shorter predicted time to failure than that associated with the lower flow stress because the initial defect size determined by the test was larger for the case with the higher flow stress. The reason for higher flow stress causing the predicted time to failure after an ILI assessment to be longer is that the initial defect size is the same irrespective of the flow

stress, but the final defect size at failure is larger for the higher-flow-stress material than final defect size associated with the lower-flow-stress material. Thus, the initial crack must grow deeper to cause a failure in the higher-flow-stress material than would be the case for the lower-flow-stress material. This implies that, in absence of knowing the actual flow stress in the case of a pipeline assessed by ILI, one should assume a low value of flow stress such as SMYS plus 10,000 psi to calculate the time to failure.

Effect of High Toughness

The effect of high toughness is examined by comparing ILI Cases 7 and 9 in Table 21.

Table 21. Effect of High Toughness on Time to Failure after an ILI Run (the compared parameter is highlighted in yellow)

ILI Case Number	Crack Depth, inch	Crack Length, inches	Half Length, inches	Predicted Failure Pressure, psig	Predicted Failure Stress, %SMYS	CVN, ft lb	Flow Stress, psi	Time to Failure, years	Cycles to Failure
7	0.040	8	4.00	1,656	101.9	20	62,000	23.8	4,341
9	0.040	8	4.00	1,733	106.7	200	62,000	24.4	4,449

It is seen in Table 21 that the case involving the higher toughness has a longer time to failure than the one involving the lower toughness. This outcome differs from the effect of toughness on time to failure after a hydrostatic test that was shown previously in Table 3. In that case the higher toughness led to a shorter predicted time to failure than that associated with the lower toughness because the initial defect sizes determined by the test were larger for the case with the higher toughness. The reason for higher toughness causing the predicted time to failure after an ILI assessment to be longer is that the initial defect size is the same irrespective of the toughness, but the final defect size at failure is larger for the higher-toughness material than final defect size associated with the lower-toughness material. Thus, the initial crack must grow deeper to cause a failure in the higher-toughness material than would be the case for the lower-toughness material. This implies that, in absence of knowing the actual toughness in the case of a pipeline assessed by ILI, one should assume a low value of toughness such as 20 ft lb to calculate the time to failure.

Effect of Tool Depth Error

When using ILI for ERW seam integrity assessment, one must recognize that there will be uncertainty associated with the dimensions provided by the service provider. To see how much effect tool depth error might have on predicted failure stress and predicted time to failure, we made the following comparisons. First, we considered the effects of 10% and 17% tool-depth errors for a relatively shallow defect (0.060-inch or 24% deep with a length of 5.5 inches) by

comparing ILI Cases 6, 10, and 11. The results are presented in Table 22. Note that the effects of the assumed errors on predicted times to failure are proportionally larger than the assumed errors themselves.

Table 22. Effects of 10% and 17% Tool Depth Errors for a 24%-Deep Defect on Times to Failure after an ILI Run (the compared parameter is highlighted in yellow)

ILI Case Number	Crack Depth, inch	Crack Length, inches	Half Length, inches	Predicted Failure Pressure, psig	Predicted Failure Stress, %SMYS	CVN, ft lb	Flow Stress, psi	Time to Failure, years	Cycles to Failure
6	0.060	5.5	2.75	1,627	100.1	20	62,000	11.2	2,055
10	0.066	5.5	2.75	1,596	98.2	20	62,000	8.8	1,610
11	0.070	5.5	2.75	1,574	96.9	20	62,000	7.5	1,368

ILI Case 6 represents the predictions based on the tool-called depth of 0.060 inch. The predicted failure stress level for this defect is 100.1 % of SMYS, and the predicted time to failure is 11.2 years. ILI Case 10 represents the situation where the depth is actually 0.066 inch, 10% deeper than the tool-called depth. In this case the predicted failure stress level is 98.2 % of SMYS, and the predicted time to failure is 8.8 years (79% of the time predicted for ILI Case 6). ILI Case 11 represents the situation where the depth is actually 0.070 inch, 17% deeper than the tool-called depth. In this case the predicted failure stress level is 96.9 % of SMYS, and the predicted time to failure is 7.5 years (67% of the time predicted for ILI Case 6). The effect on predicted failure stress is not particularly significant, but the effect on predicted time to failure is significant, and it shows that the application of a safety factor on predicted time to failure is necessary

The next two situations we examined involved a tool-call depth error of 10% for a 70%-deep defect (Table 23) and a 42%-deep defect (Table 24).

Table 23. Effect of 10% Tool Depth Error for a 70%-Deep Defect on Time to Failure after an ILI Run (the compared parameter is highlighted in yellow)

ILI Case Number	Crack Depth, inch	Crack Length, inches	Half Length, inches	Predicted Failure Pressure, psig	Predicted Failure Stress, %SMYS	CVN, ft lb	Flow Stress, psi	Time to Failure, years	Cycles to Failure
1	0.175	1.4	0.70	1,623	99.9	20	62,000	2.6	472
12	0.193	1.4	0.70	1,516	93.3	20	62,000	1.5	278

ILI Case 1 shown in Table 23 represents the predictions based on the tool-called depth of 0.175 inch. The predicted failure stress level for this defect is 99.9 % of SMYS, and the predicted time to failure is 2.6 years. ILI Case 12 represents the situation where the depth is actually 0.193

inch, 10% deeper than the tool-called depth. In this case the predicted failure stress level is 93.3 % of SMYS, and the predicted time to failure is 1.5 years (58% of the time predicted for ILI Case 1).

Table 24. Effect of 10% Tool Depth Error for a 42%-Deep Defect on Time to Failure after an ILI Run (the compared parameter is highlighted in yellow)

ILI Case Number	Crack Depth, inch	Crack Length, inches	Half Length, inches	Predicted Failure Pressure, psig	Predicted Failure Stress, %SMYS	CVN, ft lb	Flow Stress, psi	Time to Failure, years	Cycles to Failure
5	0.105	2.8	1.40	1,641	101.0	20	62,000	4.2	768
13	0.116	2.8	1.40	1,596	98.2	20	62,000	3.1	570

ILI Case 5 shown in Table 24 represents the predictions based on the tool-called depth of 0.105 inch. The predicted failure stress level for this defect is 101.0 % of SMYS, and the predicted time to failure is 4.2 years. ILI Case 13 represents the situation where the depth is actually 0.116 inch, 10% deeper than the tool-called depth. In this case the predicted failure stress level is 98.2 % of SMYS, and the predicted time to failure is 3.1 years (77% of the time predicted for ILI Case 5).

As before, the effect of tool-depth error on predicted failure stress is not overly significant, but the effect on predicted time to failure is significant. The significance of the effect becomes worse with increasing defect depth. This is because deeper, shorter defects tend to have shorter times to failure than longer, shallower defects even if the failure stress levels are the same. This was demonstrated in the presentation of times to failure after a hydrostatic test where a family of defects all having the same failure stress but varying length-depth combinations were compared..

Effect of Tool Length Error

To see how much effect tool length error might have on predicted failure stress and predicted time to failure, we made the following comparisons. First, we considered the effects of 25% tool-length error for a relatively short, deep defect (a length of 1.4 inches and a depth of 70% of the wall thickness) by comparing ILI Cases 1 and 14. The results are presented in Table 25.

Table 25. Effect of 25% Tool Length Error for a 1.4-inch-long Defect on Time to Failure after an ILI Run (the compared parameter is highlighted in yellow)

ILI Case Number	Crack Depth, inch	Crack Length, inches	Half Length, inches	Predicted Failure Pressure, psig	Predicted Failure Stress, %SMYS	CVN, ft lb	Flow Stress, psi	Time to Failure, years	Cycles to Failure
1	0.175	1.4	0.70	1,623	99.9	20	62,000	2.6	472
14	0.175	1.75	0.88	1,509	92.9	20	62,000	1.5	276

ILI Case 1 represents the predictions based on the tool-called length of 1.4 inches. The predicted failure stress level for this defect is 99.9 % of SMYS, and the predicted time to failure is 2.6 years. ILI Case 14 represents the situation where the length is actually 1.75 inches, 25% longer than the tool-called length. In this case the predicted failure stress level is 92.9 % of SMYS, and the predicted time to failure is 1.5 years (58% of the time predicted for ILI Case 1).

Next, we considered the effects of 25% tool-length error for a relatively long, shallow defect (a length of 5.5 inches and a depth of 24% of the wall thickness) by comparing ILI Cases 6 and 15. The results are presented in Table 26.

Table 26. Effect of 25% Tool Length Error for a 5.5-inch-long Defect on Time to Failure after an ILI Run (the compared parameter is highlighted in yellow)

ILI Case Number	Crack Depth, inch	Crack Length, inches	Half Length, inches	Predicted Failure Pressure, psig	Predicted Failure Stress, %SMYS	CVN, ft lb	Flow Stress, psi	Time to Failure, years	Cycles to Failure
6	0.060	5.5	2.75	1,627	100.1	20	62,000	11.2	2,055
15	0.060	6.875	3.44	1,565	96.3	20	62,000	7.2	1,312

ILI Case 6 represents the predictions based on the tool-called length of 5.5 inches. The predicted failure stress level for this defect is 100.1 % of SMYS, and the predicted time to failure is 11.2 years. ILI Case 15 represents the situation where the length is actually 6.875 inches, 25% longer than the tool-called length. In this case the predicted failure stress level is 96.3 % of SMYS, and the predicted time to failure is 7.2 years (64% of the time predicted for ILI Case 1).

Usually, tool-length errors are not as large as we assumed in these examples, but for the amount of error assumed, the effect on predicted times to failure was significant. As is the case with tool-depth error, tool-length error can have a significant effect on the predicted time to failure. As stated previously the tendency of tool error to cause uncertainty in predicted times to failure is a justification for having a factor of safety on predicted time to failure.

Conclusions Regarding the Effects of Various Fatigue Analysis Parameters on Predicted Times to Failure after an ILI Crack-Detection Tool Run

On the basis of the sensitivity study of parameters that affect the calculated times to failure after a seam integrity assessment via an ILI crack-detection tool, the following conclusions may be drawn.

1. Times to failure after an ILI seam integrity assessment that could result from fatigue crack growth can be estimated using a "Paris-law" approach, provided that the user is able to supply the relevant data that includes, pipe geometry and strength level, and the relevant operating pressure-cycle spectrum for the segment being assessed. Factors such as material toughness and flow stress can be addressed in the absence of actual data by using conservative assumptions. Satisfactory crack growth rate constants for the analysis can be found in the API 579 standard for fitness-for-service.

2. In using fatigue analysis to calculate the time to failure after a seam integrity assessment via ILI, the pipeline operator will know where defects that could grow by fatigue are located and should also be able to tell within certain bounds, the lengths and depths of the defects.

3. For a pipeline where the effective toughness of the ERW seam region is unknown, it is necessary, in the case of assessment by ILI (unlike in the case of a hydrostatic test), to assume a low value of toughness because the lower the toughness used in the analysis is, the shorter will be the predicted times to failure. In the sensitivity study herein, a toughness level corresponding to a full-size-equivalent Charpy upper shelf energy level of 20 ft lb was used for comparison to the high level of 200 ft lb. However, in conjunction with the results of the closely associated Subtask 2.4[xii] of this project it would be convenient and conservative to assume a value of 15 ft lb for the typical case where toughness is not known.

4. For a pipeline where the effective flow stress of the ERW seam region is unknown, it is necessary, in the case of assessment by ILI (unlike in the case of a hydrostatic test), to assume a low value of flow stress because the lower the flow stress used in the analysis is, the shorter will be the predicted times to failure after the test. An appropriate level of flow stress would be SMYS+10,000 psi.

5. The calculated times to failure are strongly dependent on the actual pressure cycle spectrum to which a particular location on a pipeline is subjected. Since the locations of the anomalies are known in the case of assessment by ILI, it is simply a matter of

adjusting the pressure-cycle spectrum from the upstream and active downstream stations to account for the distance along the hydraulic gradient.

6. The time to failure after an assessment by ILI is strongly dependent on the crack growth rate constants employed in the Paris-law equation. Since the actual constants that apply in a particular situation are usually unknown, the constants given in API Standard 579 may be used. Experience suggests that those constants are sufficiently conservative.

7. In the case of assessment by ILI, because the operator knows the location of each anomaly and can predict its time to failure, the operator is able to prioritize the anomalies by their times to failure and respond in a timely manner to remediate them before they grow to a size that would cause an in-service failure.

8. Because tool error may cause uncertainty as to the actual length and depth of an anomaly, the pipeline operator should take such uncertainty into account by applying a suitable factor of safety to the calculated times to failure. In cases where the times to failure were calculated for the tool-called depths and for depths 10% deeper than the tool-called depths, the times to failure were 26% to 42% shorter for the 10%-deeper defects depending on the depth/thickness ratio of the defect. In cases where times to failure were calculated for the tool-called lengths and for lengths 25% longer than the tool-called lengths, the times to failure were 37% to 42% shorter for the 25%-longer defects depending on the length of the defect.

9. Assessment of ERW seam integrity using a reliable ILI crack-detection tool should permit longer intervals between re-assessments than is the case with repeated hydrostatic testing because an ILI tool should be able to find much smaller defects than those that can survive a hydrostatic test to the highest feasible test stress levels.

FACTOR OF SAFETY

As noted previously, a factor of safety should be applied to the calculated times to failure for defects that may remain after a hydrostatic test or for specific defects that are located and sized via ILI. Typically, for the case of times to failure for defects that could have barely survived a hydrostatic, a safety factor of 2 has been applied. That is, the recommended time for retesting is half the calculated time to failure for the defect with the shortest predicted time to failure. Our experience suggests that this time to failure is adequate and appropriate. The factor of safety of 2 in this context was suggested more than 20 years ago when this type of analysis was first being applied to scheduling retesting. It was chosen somewhat arbitrarily, but with the knowledge that ASME pressure vessel design utilizes a factor of 2 on stress to avoid fatigue failures in service.

The fact that ASME practice is to apply a factor of 20 on cycles to failure was not seen as a practical approach for fatigue crack growth in pipelines because the ASME practice applies to crack initiation not crack propagation. That is, fatigue life in the context of pressure vessel design envisions the cyclic life of a defect-free structure where most of the fatigue life involves the initiation of a crack. It is believed that the factor of safety of 20 was instituted to account for the possibility that an as-built structure might not in fact be defect-free. In contrast, the fatigue-life prediction method for pipelines is based on a known initial defect size, and the uncertainty involved in the calculation is believed to be much more limited.

The appropriate factor of safety for the calculated times to failure for defects identified and characterized by ILI is 2 if tool error is accounted for in some way. It is known that at least one ILI service provider calculates remaining lives using a factor of safety of 2 (meaning that a response to an anomaly should be carried out by the time half the time to failure has expired), but there are other inherent safety factors in the calculations. For one thing, this particular service provider assumes the depth to be the upper limit of each "bracket" of depth. The tool calls are generally given as ranges or brackets (e.g., less than 12.5 % of the wall thickness, 12.5% to 25% of the wall thickness, 25% to 40% of the wall thickness, greater than 40% of the wall thickness). The analysis of a defect in the 25% to 40% bracket would be based on a depth of 40%, for example. If the depth exceeds 40%, the analyst would probably assume a depth of at least 50% of the wall thickness. In some cases a tool tolerance is added to the depth of the anomaly as well. Offsetting these built-in conservatisms, this particular service provider uses a *C* value of 3.6E-19[6] instead of the value of 8.61E-19 suggested in this document. As the life is proportional to the *C* value, this means that the service provider's times to failure are 2.4 times longer than those that would be predicted using the *C* value suggested in this document. Using a factor of safety of 2 with some additional conservatism built in (e.g., assuming the deepest depth in the bracket, adding a specific tool tolerance) would seem to be satisfactory if used in conjunction with a *C* value of 8.61E-19.

DISCUSSION

This study has shown that times to failure after a hydrostatic test can be calculated via Paris-law approach, provided that the analyst is able to supply the relevant data that includes, pipe geometry and strength level, the relevant operating pressure-cycle spectrum and test pressure

[6] The value of 3.6E-19 has been experimentally verified for ferrite-pearlite steel base metal as can be ascertained from Reference ix, Page 202. The API 579 standard mentions that as well. However, the API 579 standard recommends the value of 8.61E-19 for weld metal such as a submerged-arc weld in a pipe or pressure vessel. We have chosen to apply the latter value instead of the former value because the bondline region of an ERW seam is non-homogeneous and thus potentially more likely to be more susceptible to crack growth than the base metal of the pipe..

history for the segment being assessed. Other factors that affect the times to failure include material toughness, flow stress, and the crack growth rate constants associated with the Paris-law equation. These latter factors will not be known for each and every piece of pipe in a pipeline. However, the sensitivity analysis shows that the analyst can expect to obtain conservative estimates of times to failure after a hydrostatic test by assuming a toughness level corresponding to a full-size-equivalent Charpy upper-shelf energy level of 200 ft lb and a flow stress equal to the minimum specified ultimate tensile strength of the base metal. Experience shows that the crack growth rate constants found in the API 579 standard for fitness-for-service are acceptable. Lastly, a factor of safety of 2 should be applied to the calculated times to failure to account for uncertainties in the material properties and the calculation process.

In using fatigue analysis to calculate the times to failure after a hydrostatic test, it must be assumed that defects could exist anywhere along the pipeline that are severe enough to have failure pressures no higher than that of the hydrostatic test pressure. This means that the analyst may have to calculate times to failure for multiple points along the pipeline taking account of the test level applied at each location, the wall thickness at each location, the effect of the hydraulic gradient on the pressure cycles at each location, and the effect of elevation on the static head at each location.

The sensitivity study further shows that the calculated times to failure after a hydrostatic test increase exponentially with increasing test-pressure-to-operating-pressure ratio. Therefore, the operator can maximize the length of time between retests by utilizing the highest feasible test pressure the will not cause significant permanent expansion of pipe or an intolerable number of test failures. For a pipeline that is operated at maximum stress levels below 72% of SMYS, the test-pressure-to-operating-pressure ratio must be greater than that applied on a pipeline that operates at 72% of SMYS to achieve the same time to failure as that for the pipeline that operates at 72% of SMYS.

The sensitivity study also addressed the parameters that affect the calculated times to failure after a seam integrity assessment via an ILI crack-detection tool. In a manner similar to that used to calculate times to failure after a hydrostatic test, times to failure after an ILI seam integrity assessment can be estimated using a “Paris-law” approach. For an analysis following seam assessment by ILI, the user must know the pipe geometry and strength level, and the relevant operating pressure-cycle spectrum for the segment being assessed. In the case of assessment by ILI (unlike in the case of a hydrostatic test), it is prudent to assume a low value of toughness because the lower the toughness used in the analysis is, the shorter will be the predicted times to failure. A toughness level corresponding to a full-size-equivalent Charpy upper shelf energy level of 15 ft lb would seem to be an appropriate value.

Also, unlike in the case of a hydrostatic test, it is prudent to assume a low value of flow stress because the lower the flow stress used in the analysis is, the shorter will be the predicted times to failure after the test. An appropriate level of flow stress would be SMYS+10,000 psi.

As in the case involving predicting times to failure after a hydrostatic testing, the crack growth rate constants found in the API 579 standard for fitness-for-service are acceptable for use in calculating times to failure after a seam assessment via ILI.

In using fatigue analysis to calculate the time to failure after a seam integrity assessment via ILI, the pipeline operator will know where defects that could grow by fatigue are located and should also be able to tell within certain bounds, the lengths and depths of the defects. Since the locations of the anomalies are known in the case of assessment by ILI, it is simply a matter of adjusting the pressure-cycle spectrum from the upstream and active downstream stations to account for the distance along the hydraulic gradient. An analysis should be made for all significant anomalies so that the times to failure will be known. The operator will then be able to prioritize the anomalies by their times to failure and respond in a timely manner to remediate them before they grow to a size that would cause an in-service failure.

Assessment of ERW seam integrity using a reliable ILI crack-detection tool should permit longer intervals between re-assessments than is the case with repeated hydrostatic testing because an ILI tool should be able to find much smaller defects than those that can survive a hydrostatic test to the highest feasible test stress levels.

The sensitivity study reveals that errors in tool-called depth can significantly alter the time to failure. In cases where the times to failure were calculated for the tool-called depths and for depths 10% deeper than the tool-called depths, the times to failure were 26% to 42% shorter for the 10% deeper defects depending on the depth/thickness ratio of the defect. In cases where times to failure were calculated for the tool-called lengths and for lengths 25% longer than the tool-called lengths, the times to failure were 37% to 42% shorter for the 25% longer defects depending on the length of the defect. Because tool error may cause uncertainty as to the actual length and depth of an anomaly, the pipeline operator should take such uncertainty into account by applying a suitable factor of safety to the calculated times to failure. As was discussed previously, applying a factor of safety of 2 with some additional conservatism built in (e.g., assuming the deepest depth in the bracket, adding a specific tool tolerance) would seem to be satisfactory.

REFERENCES

[i] Kiefner, J.F., and Kolovich, K.M., "*ERW and Flash Weld Seam Failures*" Subtask 1.4 of U.S. Department of Transportation Other Transaction Agreement No. DTPH56-11-T-000003, May 30, 2012.

[ii] Paris, P.C., and Erdogan, F., "*A Critical Analysis of Crack Propagation Laws*", Transactions of ASME, Journal of Basis Engineering, Series D, Volume 85, No. 5, (1963) pp 405-09

[iii] J.C. Newman, Jr. and I.S. Raju, "An Empirical Stress-Intensity Factor Equation for the Surface Crack". *Engineering Fracture Mechanics,* Vol. 15, No. 1-2, pp 185-192, 1981, printed in Great Britain.

iv Kiefner, J.F., "Modified equation helps integrity management", Oil and Gas Journal, Oct 6, 2008, pp 76-82 and "Modified Ln-Secant equation improves failure prediction"Oct 13, 2008, pp 64-66.

[v] Leis, B. N., Brust, F. W., and Scott, P.M., "Development and Validation of a Ductile Flaw Growth Analysis for Gas Transmission Line Pipe", Final Report to American Gas Association, NG-18, Catalog No, L51543, 1991.

[vi] Jaske, C. E., and Beavers, J. A., "Development and Evaluation of Improved Model for Engineering Critical Assessment of Pipelines", Proceedings of IPC 2002, 4th International Pipeline Conference, September 29-October 3, 2002, Calgary, Alberta, Canada

[vii] Anderson, T. L., Merrick, R. D., Yukawa, S., Bray, D. E., Kaley, L., and Van Scyoc, K., "*Fitness-For-Service Evaluation Procedures For Operating Pressure Vessels, Tanks, And Piping in Refinery And Chemical Service*", FS-26, Consultants' Report, MPC Program On Fitness-For-Service, Draft 5, The Materials Properties Council, New York, N.Y., October, 1995.

[viii] API 579-2/ASME FFS-1 – Fitness-for-Service, 2009

[ix] Barsom, J.M., and Rolfe, S.T., *Fracture and Fatigue Control in Structures: Applications of Fracture Mechanics,* Third Edition, ASTM Stock Number MNL41, 1999.

[x] Mayfield, M.E., and Maxey, W.A., "*ERW Weld Zone Characteristics*". Final Report to A.G.A./PRC, A.G.A. Catalog No. L51427, June, 1982.

[xi] Kiefner, J.F., Kolovich, C.E., Zelenak, P.A., and Wahjudi, T., "Estimating Fatigue Life for Pipeline Integrity Management", IPC04-0167, *Proceedings of IPC 2004 International Pipeline Conference*, Calgary, Alberta, Canada (October 4-8, 2004).

[xii] Kiefner, J.F., and Kolovich, K.M., "*Models for Predicting Failure Stress Levels for ERW and Flash Weld Seams*" Subtask 2.4 of U.S. Department of Transportation Other Transaction Agreement No. DTPH56-11-T-000003, December 18, 2012.